ACTIVE VIBRATION CONTROL OF SHELL

A DISSERTATION

Submitted in partial fulfillment of the
requirements for the award of the degree
of
MASTER OF TECHNOLOGY
in
MECHANICAL ENGINEERING
(With Specialization in Machine Design Engineering)

By

ANURAG SHARMA

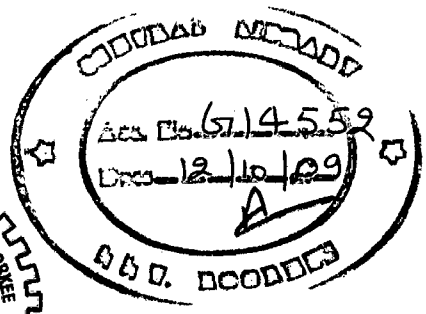

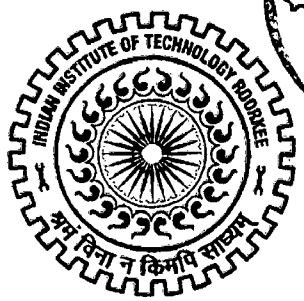

DEPARTMENT OF MECHANICAL AND INDUSTRIAL ENGINEERING
INDIAN INSTITUTE OF TECHNOLOGY ROORKEE
ROORKEE - 247 667 (INDIA)
JUNE, 2009

INDIAN INSTITUTE OF TECHNOLOGY ROORKEE

ROORKEE

CANDIDATE'S DECLARATION

I here by declare that the work, which is being presented in this dissertation titled **"ACTIVE VIBRATION CONTROL OF SHELL"** in the partial fulfillment of the requirement for the award of the degree of **Master of Technology** with specialization in **Machine Design Engineering**, submitted in **Mechanical & Industrial Engineering India Institute of Technology Roorkee, India**, is an authentic record of my own work carried out during the period from june 2008 to june 2009, under the supervision of Dr. S. C. Jain, Professor and Dr. B.K. Mishra, Professor, MIED, IIT Roorkee, India.

I have not submitted the matter embodied in this dissertation for the award of any other degree or diploma.

Date: 29/06/09

Place: **Roorkee**

(Anurag Sharma)

CERTIFICATION

This is to certify that the above statement made by the candidate is correct to the best of our knowledge and belief.

(Dr. B. K. Mishra)
Professor,
MIED
IIT Roorkee, India

(Dr. S. C. Jain)
Professor,
MIED
IIT Roorkee, India

Date: 29/06/09

Place: **Roorkee**

ACKONWLEDGEMENT

I am highly indebted to **Dr. S. C. Jain, Professor & Dr. B. K. Mishra, Profressor**, Department of Mechanical & Industrial Engineering, Indian Institute of Technology Roorkee, India for encouraging me to undertake this dissertation as well as providing me all the necessary guidance and inspirational support throughout this dissertation work. They had displayed unique tolerance and understanding at every step of progress. It is my proud privilege to have carried the dissertation work under able guidance of them.

I am very grateful to **Dr. Pradeep kumar, Professor,** Head of the department of Mechanical and Industrial engineering, who supported my effort.

I also thank **Dr. S. P. Harsha**, Assistant Professor, MIED for his valuable suggestions and fruitful discussions related to this work and also for providing me a chance to work in vibrations and automation laboratory. I would also like to thanks the technical as well as non technical staff of vibrations and automation laboratory and tin smithy shop, Mechanical & Industrial Engineering for all their help and support.

I express my gratitude to all teachers of the department who had been source of inspiration to me.

I express my regards to my parents and brother who have been a constant source of inspiration to me. Finally I would like to thank all my friends, for their help and encouragement at the hour of need.

(Anurag Sharma)
M. Tech (Machine design) IInd year
I. I. T. Roorkee, India

CONTENTS

Recent advances in materials science have led to the development of a range of functional materials which when embedded into a structure can produce and monitor structural deformations. These structures have been labeled 'smart structures' and such materials are known as 'smart materials'. Smart materials have the ability to change shape or size dramatically thus have the capability to 'feel' a stimulus and suitably react to it just like any living organism. Each individual type of smart material has a different property which can be significantly altered, such as viscosity, volume, and conductivity. The property that can be significantly altered influences the likely applications of the smart material.

In the recent years, there has been great interest among engineers to builds 'smart structure' that have capability of sensing and actuating in a controlled manner in response to an input and adjust their properties and shapes to the changing environment. The adjustments in such structures may be made through the use of actuators. The attenuation of vibrations is a problem of primary importance in many engineering fields, particularly so in aerospace applications. This work deals with the experimental assessment of suppression of vibration using piezoelectric patches as smart material. These patches are usually thin wafers, which are poled in the thickness direction and bonded to the surfaces of the host structures. Piezoelectric material such as PZT patch (Piezoceramic patch) is equally effective as sensor and actuator. PZT patch is useful in vibration control because of advantages of high stiffness, light weight, low power consumption and easy implementation.PZT patches are considered to be bonded on the top and bottom surfaces of the host structure. These patches act as sensors and actuators.

An experimental setup has been fabricated to demonstrate the use of piezoelectric material like PZT patch in the active vibration control application. This setup includes the piezoelectric material i.e. PZT patches, data acquisition card, signal conditioner and a computer with LabVIEW software. The aluminum semi-circular cylindrical shell is mounted in the cantilever configuration and excited manually by tapping. The vibration of the shell is controlled by the piezo actuation system by increasing the gain. Control strategies such as proportional control have been implemented. In the control strategies, the feedback voltage is generated as a function of position quantities. As the shell deforms, due to external applied loads, the bonded piezoelectric film (sensor) also

deforms, and due to its constitutive behavior, it develops a voltage proportional to the applied force. The voltage is then amplified by a control system, to obtain the feedback voltage. This feedback voltage is supplied to the other piezoelectric film (actuator) that induces a counteractive deformation to the shell structure and the amplitude of vibration is suppressed.

Notation	Definition
$[B_u]$	Strain displacement matrix
$[C_{uu}]_e$	Structural damping matrix
$\{D\}$	Electrical displacement
$\{E\}$	Electric field
e_{3i}	Unit vector normal to the mid-surface
e_{1i} & e_{2i}	Orthogonal directions tangential to the plane
$[e_p]$ & $[e_t]$	Piezoelectric stress constants
$\{F_\varphi\}_e$	Force vector
$\{F_q\}_e$	Mechanical load
h_i	Nodal thickness of the element.
J	Jacobian
J'	Inverse jacobian
$[K_{uu}]_e$	Stiffness matrix
$[K_{u\varphi}]_e$	Electromechanical coupling stiffness matrix
$[K_{\varphi\varphi}]_e$	Dielectric stiffness matrix
$[M_{uu}]_e$	Element mass matrix
Ni	Quadratic shape function
$\{q\}_e$	Nodal displacement vector.
$[Q_p]$	Stress reduced elasticity matrix
$[Q_t]$	Transverse shear elasticity matrix
u_i	Nodal displacements in x directions
v_i	Nodal displacements in y directions
w_i	Nodal displacements in z directions

Coordinate system

x, y, z	Global coordinate system
x',y',z'	Local coordinate system
ξ,η,ς	Natural coordinate system
l_{1i} , $m_{1i,}$ n_{1i}	Direction cosine between local z' axes to global axes x, y, z

$l_{2i,}$ m_{2i}, n_{2i}	Direction cosine between local z' axes to global axes x, y, z
l_{3i}, m_{3i}, n_{3i}	Direction cosine between local z' axes to global axes x, y, z

Greek symbols

σ_p	Stress components
τ_t	Shear stress components
ε_p & γ_t	Corresponding strains
ε'	Local strains
ξ	Natural coordinate in x direction
η	Natural coordinate in y direction
ζ	Natural coordinate in z direction
ϵ	Permittivity coefficient
ρ	Material density
θ_{xi}	Rotation about x axis
θ_{yi}	Rotation about y axis

Subscripts

a	Actuator
e	Element
s	Sensor
u	Elastic
θ	Temperature
Ø	Electric
x	x direction
y	y direction
z	z direction
x'	Local-running coordinate system in x direction
y'	Local-running coordinate system in x direction
z'	Local-running coordinate system in x direction
i	Node number

Superscripts

T	Transpose of matrix
e	Element
. (dot)	First derivative w.r.t time
.. (double dot)	Double derivative w.r.t time

LIST OF FIGURES

LIST OF TABLE

Chapter 1

INTRODUCTION

1.1 Motivation

Vibration analysis and control of a structure are among the major research subjects in mechanical, aerospace, civil engineering and other related disciplines and are vital for many industrial applications. Structural damping refers to the capacity of a structure or structural component to dissipate energy or to its capacity for removing, from the structural vibration, some of the energy associated with that vibration. This removed energy may be converted directly to heat and transferred to connected structure or to the ambient media.

Recent studies on smart structures have shown that piezoelectric materials can be effective alternative to the conventional discrete sensing and control systems. Piezoelectric materials have coupled mechanical and electrical properties. They generate an electrical charge when subjected to a mechanical deformation, a property called direct piezoelectric effect. Conversely, mechanical stress or strain is produced by an applied electric field, which is called the converse piezoelectric effect. Bonded or embedded piezoelectric patches in a structure can act as sensors to monitor or as actuators to control the response of the structure. The ability of piezoelectric materials is to transform mechanical energy into electrical energy and vice versa makes them suitable for both the sensor and actuator applications. Other advantages include: simple integration into the structure; a readily obtainable commercial supply of piezopolymers and piezoceramic. The two common types of piezoelectric materials are lead zirconate titanate (PZT) ceramics and polyvinylidene fluoride (PVDF) polymers.

Of these different types of actuators available, piezo electric actuators that are surface mounted or embedded provide a promising smart material control system due their low cost, space efficient characteristics, fast response, large force output, being inexpensive and light weight.

Most of the engineering materials such as steel, aluminum and other metals have very little inherent damping. Hence structures, built by using such materials, in general, have vibration problems, particularly near resonance frequencies, which could cause an unpleasant noise and premature fatigue failure of the components. Thus there is a need to

apply some external damping mechanism, to these structures, to control the vibration level under acceptable limits.

1.2 Preamble

The primary objective of this study is to develop an experimental setup to demonstrate the use of piezoelectric material like PZT patch in the active vibration control application. This setup includes the piezoelectric material i.e. PZT patches, data acquisition card, signal conditioner and a computer with LabVIEW software. The aluminum semi-circular cylindrical shell is mounted in the cantilever configuration and excited manually by tapping. The vibration of the shell is controlled by the piezo actuation system by increasing the gain. In the control strategies, the feedback voltage is generated as a function of position quantities. As the shell deforms, due to external applied loads, the bonded piezoelectric film (sensor) also deforms, and due to its constitutive behavior, it develops a voltage proportional to the strain. The voltage is then amplified by a control system, to obtain the feedback voltage. This feedback voltage is supplied to the other piezoelectric film (actuator) that induces a counteractive deformation to the shell structure and the amplitude of vibration is suppressed.

1.3 Organization of the thesis

Chapter 2 explains the background of the smart materials and piezoelectric material. Strategies of the active vibration control have been discussed.

Chapter 3 contains a brief discussion regarding the previous work that has been done in this field. A Summary of work carried out by different authors, their objectives and conclusions are presented in this chapter.

Chapter 4 details the development of the finite element model. The derivation of the equations of motion with sensor and actuator equations are given in detail. Control strategies used in the present work are also discussed.

Chapter 5 describes the experimental setup for the active vibration control. This includes the specification of the apparatus used in the experimental setup and their uses in the experiment. Procedure of active vibration control is also explained.

Chapter 6 presents the results and discussion of the present work. The controlled and uncontrolled responses of cantilever semi-circular cylindrical shell are compared numerically and experimentally.

Chapter 7 presents the conclusion of the present work and scope for future work.

Chapter 2

BACKGROUND

This chapter gives an introduction of the smart material in general along with a description of piezoelectric material. It also covers the active vibration control strategies for the vibration suppression.

2.1 Smart material

Science and technology have made amazing developments in the design of electronics and machinery using standard materials, which do not have any particularly special properties. These special materials have properties which can be manipulate by scientists and engineers. Some such materials have the ability to change shape or size dramatically simply by adding or removing a little bit of energy. These materials are called smart materials. Smart materials have one or more properties that can be dramatically altered such as viscosity, volume, and conductivity. The property that can be altered influences the likely types of applications of the smart material. Varieties of smart materials already exist, and are being researched extensively.

In the recent years, there has been great interest among engineers to builds "smart" structure that have capability to adjust their properties and shapes to the changing environment. The adjustments in such structures may be made through the use of actuators. The attenuation of vibrations is a problem of primary importance in many engineering fields, particularly so in aerospace applications.

Smart structure can be defined as structures that are capable of sensing and actuating in a controlled manner in response to an input. As system elements become more lightweight, to satisfy inertia and size requirements, vibration can become a prominent factor in their dynamic behavior. This vibration is undesirable and active control methods are required to modify the dynamic response. Many of the devices used for passive damping are large, heavy and unsuitable for lightweight applications. Recent advances in materials science have led to a range of functional materials that, when embedded into a structure can produce and/or monitor structural deformations. These structures have been labeled 'smart structures'. Active vibration control methods can be

used to eliminate the undesired vibrations. The use of the smart structure is having tremendous growth in controlling the vibration and shape of the structure.

Smart materials play very important role to control the vibration in such structure. These include piezoelectric materials, magneto-rheostatic materials, electro-rheostatic materials, and shape memory alloys.

2.2 Piezoelectric Material

Piezoelectric materials have the unique ability to interchange electrical energy and mechanical strain energy or force. Due to this characteristic of the material, it has been found to be very effective for use in dynamic applications involving vibration suppression and sensing. While these materials have found notable applications such as high voltage generators for gas lighters ,fuses for explosives, ultrasonic cleaners, welders and atomizers, strain and excitation gauges, accelerometers, transducers, flow meters, dynamic force and pressure measurement, sonar, deepwater hydrophones and piezoelectric actuators/translators.

In 1880, the first experiment displaying the piezoelectric effect was performed on specially prepared crystals (quartz, topaz, tourmaline, cane sugar and Rochelle salt) and published by Pierre and Jacques Curie. While the Currie brothers were able to predict that electricity could be generated from an applied stress (direct piezoelectricity), they did not predict the opposite effect, know as converse piezoelectricity. Direct piezoelectricity illustrates that when a mechanical stress is applied to the material an electric charge results, this converse phenomena illustrates that the application of an electrical field creates a mechanical stress. The converse piezoelectric effect was later mathematically proven in 1881 by Lippman using the fundamental thermodynamic principles. The converse piezoelectric effect was quickly confirmed by the Curies and quantitative proof of the complete reversibility of electro-elasto-mechanical deformations in piezoelectric crystals was later obtained. After its discovery and until the early 1900's, piezoelectricity was mainly a topic of scientific interest. The early twentieth century was producing many new machines, none of which incorporated piezoelectricity. The reason for the lack of applications was primarily because piezoelectricity was an obscure science and the recently developed mathematics describing this phenomenon were very complicated and hard to understand. However, in 1916 during World War I, Paul Langevin of France developed the first engineering use

for piezoelectricity by developing an ultrasonic submarine detector. From 1917 through the 1940's Cady's work as well as others led to a period of intense development of piezoelectric devices. During this period of intense piezoelectric research, numerous applications were developed that we now find common including microphones, accelerometers, ultrasonic transducers, bender element actuators and phonograph pick-ups. In the beginning of the mid 1930's, there were some advances in the production of materials with higher piezoelectric properties, leading to the development of the crystal ADP (ammonium dihydrogen- phosphate). ADP possessed the rugged characteristic of the quartz crystal and the strong piezoelectric characteristics of Rochelle salt In addition to ADP several other piezoelectric crystals were identified, a few of the more effective ones are EDT (ethylene diamine tartrate), DKT (dipotoassium tartrate) and BaTiO3 (Barium Titanium Oxide). The advances made in these crystals lead to the development of wave filters for use in multichannel telephony work at Bell telephone Laboratories. The next step in the development of high performance piezoelectric materials occurred during World War II. In the U.S., Japan and the Soviet Union, isolated research groups were developing advanced capacitor materials and found that certain ceramics prepared by sintering metallic oxide powders, exhibited dielectric constants up to 100 times greater than those of the commonly cut crystals of the time. This discovery of an easily manufactured piezoelectric ceramic with far greater performance than any other to date sparked a new period of intense research and development of piezoelectric devices. The greater research efforts began to produce ceramic materials with better piezoelectric properties than Barium titanate, leading to the development of numerous materials, the most notable of these being lead metaniobate (PMN) and lead zerconate titanate (PZT). These two materials are still among the most used for piezoelectric applications today. Following the development of the piezoceramic was the piezoelectric semiconductor film and piezoelectric polymers. The most notable of the piezo-polymers is the polyvinylidene fluoride film (PVDF), which is still heavily used.

2.3 Active Vibration Control

The structure is seen as a system with vibratory loads applied as inputs to the system. Then the problem is carried out in the form of a control strategy i.e. the reduction of the undesired output effects by means, for an example, of a classic feedback closed loop with its sensing and actuating devices. A structure in which the damping action is realized by automatic control techniques is named "controlled structure" and it is a

Chapter 3

LITERATURE REVIEW

This chapter presents the literature review regarding active vibration control of structures.

3.1 Smart Material

Thomson et al. [1992] presented an exposition of the embryonic field of smart materials and structures. They discussed different classes of innovative biomimetic materials and their influence on design practices.

Brennan et al. [1994] presented the use of piezoelectric elements as vibration actuators and sensors on a one dimensional structure. They developed an analytical model to describe how piezoelectric sensors and actuators measure and excite longitudinal and flexural waves on a beam and validated it with simple experiments. They stated the merits of using these elements as error sensors and as an secondary source of active vibration control system and also highlighted some fundamental limitations.

Akella et al. [1994] presented the modeling and control issues related to smart structures bonded with piezoelectric sensors and actuators. They firstly apply Hamilton's principle to obtain a linearized equation of motion and then they found natural modes by solving an eigenvalue problem.

Bronowicki et al. [1995] fabricated a member with thin PZT actuator and sensor wafers embedded in the composite layup and then this member is subjected to cyclic loading. They found that the product of PZT modulus and piezoelectric coefficient is a figure of merit for both actuation and sensing.

3.2 Analysis of shell

Aida et al. [1998] presented study of a new shell type dynamic vibration absorber for suppressing several modes of vibration of the shallow shell under harmonic load and also presented formulae for an approximate tuning method for the shell type dynamic absorber using the optimum tuning method for a dynamic absorber in the two degree of freedom system obtained by the Den Hartog method. They also presented

particular case of a more general class named "active structures", for which either a sensitive or an actuative component is present.

More than a decade of intensive research in the area of smart/adaptive structures has demonstrated the viability and potential of this technology. A class of smart structures, consisting of piezoelectric materials integrated with structural systems, has found widespread use in engineering applications, including active vibration suppression. Piezoelectric actuators used in adaptive structures are usually thin wafers, which are poled in the thickness direction and bonded to the surfaces of the host structure. The application of an electric field in the thickness direction causes the lateral dimensions of the actuators to increase or decrease, thereby forcing the host structure to deform. These types of actuators, where the electric field is applied parallel to the poling direction to cause normal strains in the piezoelectric material, are known as piezoelectric extension actuators. Piezoelectric extension actuators are usually placed at the extreme thickness positions of a semi-circular cylindrical shell-like structure to achieve the most effective actuation.

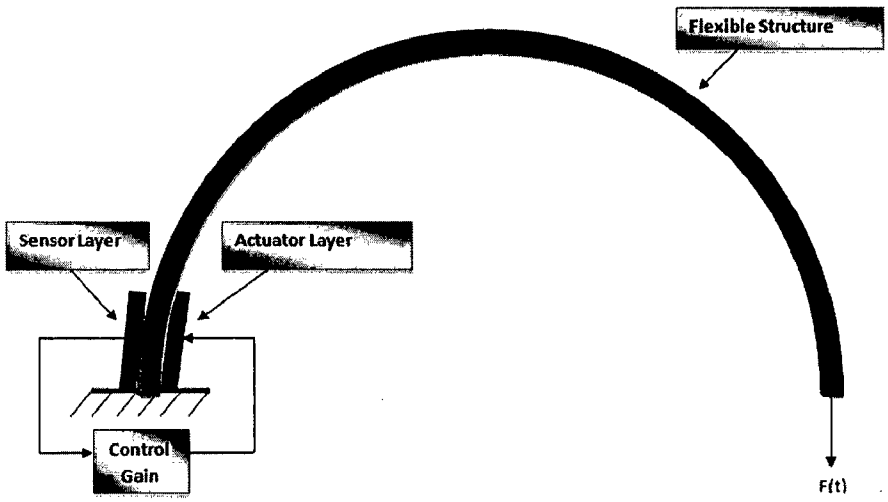

Figure 2.1: An active control system

Figure 2.1 typically shows the active vibration control system. It consists of the sensor which is used to monitor the mechanical response of the structure through strain, acceleration or velocity etc. The adverse or undesirable signal sensed by the sensor is used in controller to send the corrected signal to the actuators.

Chapter 3

LITERATURE REVIEW

This chapter presents the literature review regarding active vibration control of structures.

3.1 Smart Material

Thomson et al. [1992] presented an exposition of the embryonic field of smart materials and structures. They discussed different classes of innovative biomimetic materials and their influence on design practices.

Brennan et al. [1994] presented the use of piezoelectric elements as vibration actuators and sensors on a one dimensional structure. They developed an analytical model to describe how piezoelectric sensors and actuators measure and excite longitudinal and flexural waves on a beam and validated it with simple experiments. They stated the merits of using these elements as error sensors and as an secondary source of active vibration control system and also highlighted some fundamental limitations.

Akella et al. [1994] presented the modeling and control issues related to smart structures bonded with piezoelectric sensors and actuators. They firstly apply Hamilton's principle to obtain a linearized equation of motion and then they found natural modes by solving an eigenvalue problem.

Bronowicki et al. [1995] fabricated a member with thin PZT actuator and sensor wafers embedded in the composite layup and then this member is subjected to cyclic loading. They found that the product of PZT modulus and piezoelectric coefficient is a figure of merit for both actuation and sensing.

3.2 Analysis of shell

Aida et al. [1998] presented study of a new shell type dynamic vibration absorber for suppressing several modes of vibration of the shallow shell under harmonic load and also presented formulae for an approximate tuning method for the shell type dynamic absorber using the optimum tuning method for a dynamic absorber in the two degree of freedom system obtained by the Den Hartog method. They also presented

numerical calculations which demonstrate the usefulness of the shell type dynamic vibration absorbers.

Young et al. [2000] presented a three-dimensional shell theory which is applicable to doubly curved thick open shells which are arbitrarily deep in one principal direction but are shallow in the other direction. They expressed strain-displacement equations in Cartesian co-ordinates and discussed the limits of these equations .Using these equation they found natural frequencies of a number of doubly curved shell problems and proposed a novel approach in which penalty functions are introduced to enforce continuity of displacements at two opposite ends of a shell of rectangular platform.

Ye et al. [2000] developed a numerical method to investigate the complicated temperature, mechanical, and control interactions of piezothermoelastic shell composites and formulated a new piezothermoelastic composite triangular element. They used electric force vector to active control shell laminates and compared finite element solutions of a piezoelectric laminated composite plate with experimental data and numerical solutions.

Moussoui et al.[2002] provided a contemporarily relevant survey of studies on non-linear vibrations of shell-type structures and presented the effects of geometrical non-linearity and specific difficulties encountered in non-linear dynamic analysis of shell-type structures. They Comments on the previous non-linear works are presented and some orientations for future research are suggested.

Narayanan et al. [2003] presented finite element modeling of laminated structures with distributed piezoelectric sensor and actuator layers and control electronics and develop beam, plate and shell type elements incorporating the stiffness, mass and electromechanical coupling effects of the piezoelectric laminates. They used Constant-gain negative velocity feedback, Lyapunov feedback as well as a linear quadratic regulator approach for active vibration control with the structures subjected to impact, harmonic and random excitations and investigated the influence of the pyroelectric effects on the vibration control performance. They found that LQR approach is more effective in vibration control with lesser peak voltages applied in the piezo- actuator layers.

Awrejcewicz et al. [2003] analyzed orthotropic plates and shells with variable thickness and low transverse stiffness. Then discussed the finite approximation of the problem related to optimization of free vibrations of shells with transverse deformation

and rotary inertia. Their convergence and suitability for application to plates and shells analysis are discussed and numerically evaluated.

Berg et al. [2004] present new equations of motion for the vibration of piezo-ceramic thin-walled cylindrical shells, generalizing flugge shell theory for this type of material. These new equations differ from the ones known from the literature is that here the electric field is not assumed as constant over the thickness but is obtained by solving an additional differential equation in the thickness direction.

Lee et al. [2006] presented the natural frequencies of isotropic and composite laminates and investigated the forced vibration analysis of laminated composite plates and shells subjected to arbitrary loading. They used the Mindlin-Reissner theory which allows the shear deformation and rotary inertia for development of nine-node assumed strain shell element. Their results show good agreement with the 3-D elasticity and analytical solutions. In addition they also investigated the effect of damping on the forced vibration analysis of laminated composite plates and shells.

Yue et al. [2007] focuses on spatially distributed modal sensing characteristics of free-floating flexible paraboloidal membrane shells laminated with distributed sensor patches based on a new set of assumed mode shape functions. They evaluate overall sensing/control affects, microscopic sensing signal characteristic, sensor segmentation and location of distributed sensors on thin paraboloidal membrane shells with different curvatures. They suggested that the signal generation depends on modal membrane strains in the meridiona and circumferential.

Liu [2007] et al. presented the implementation of the element free Galerkin method for static and free vibration analysis of general shell structures. They constructed a discrete singularity-free mapping between the five- and the six-degrees-of-freedom by exploiting the geometry connection between the orthogonal group and the unit sphere and used moving least-squares approximation in both the construction of shape functions based on arbitrarily distributed nodes as well as in the surface approximation of general spatial shell geometry.

Van et al. [2008] presents numerical analyses of free vibration of laminated composite plate/shell structures of various shapes, span-to-thickness ratios, boundary conditions and lay-up sequences. They built element by incorporating a strain smoothing method into the bilinear four-node quadrilateral finite element where the strain

smoothing operation is based on mesh-free conforming nodal integration and demonstrated several numerical examples about the capability, efficiency and simplicity of the element and compare with other existing solutions in the literature, suggest that the present element is robust, computationally inexpensive and free of locking.

Ansari et al. [2008] presents a general analytical approach to investigate vibrational behavior of functionally graded shells. The theoretical formulations is based on first order shear deformation shell theory, take into consideration transverse shear deformation and rotary inertia effects. They studied the influence of some commonly used boundary conditions, the effect of variations of volume fractions and shell geometrical parameters on the vibration characteristics. The results show good agreement with those available in the literature.

Roy et al. [2009] presented an improved genetic algorithm (GA) based optimal vibration control of smart fiber reinforced polymer (FRP) composite shell structures and formulated layered shell finite elements and the formulation has been validated for coupled electromechanical analysis of curved smart FRP composite structures having piezoelectric sensors and actuators patches. They used integer-coded GA-based open-loop procedure for optimal placement of actuators for maximizing controllability index and implemented a real coded GA-based linear quadratic regulator (LQR) control scheme for optimal control of the smart shell structures in order to maximize the closed-loop damping ratio while keeping actuators voltages within the limit of breakdown voltage. Results show that this combined GA based optimal actuators placement and GA-based LQR control scheme is far superior to conventional active vibration control using LQR schemes and simple placement of actuators reported in literatures.

3.3 Optimal Sensor/Actuator Placement

Obe [1985] proposed a scheme for the optimal spatial placement of a limited number of sensors and actuators under a minimum energy requirement for active control of flexible structures. The method was based on the interpretation of the functional relationship between the actuators and the modes of the structural system. He showed that from the form of the matrix, the controllability and the observability of the system with respect to differing locations of sensors and actuators can be established. The algorithm presented circumvents prevailing problems encountered in contemporary

optimal control applications. In order to support the conclusions, numerical simulation for a prismatic beam subjected to horizontal random wind loads and simply supported square plate modeled as single degree of freedom system were provided.

Tzou et al. [1992] studied a new intelligent shell structure composed of a conventional elastic shell, a distributed piezoelectric sensor & actuator and derived system equations of motion coupling sensing and control effects, from the theory derived, it is concluded that the distributed sensor is capable of sensing all shell vibration modes and the distributed actuator controlling all shell modes.

Hiramoto et al. [2000] presented an optimal sensor and actuator placement strategy for active vibration control of flexible structures. They obtained two solutions of generalized algebraic Riccati equations for undamped structure with collocated sensors and actuators. Employing the explicit solution, they obtained a stabilizing controller based on normalized coprime factorization approach without solving any algebraic Riccati equations numerically. They showed that the amount of computation required determining the optimal sensor/actuator placement and controller gain increases rapidly for large scale structures. They automatically bounded the closed loop property on the stabilizing norm for all candidates of optimal placement. Hence the optimal sensor/actuator placement problem was formulated to optimize other closed loop properties with less computation required than the model based method. Using the sensitivity formula, they obtained the optimal placement of the two pairs of sensors and actuators which minimize the stabilizing norm of closed loop system for a simply supported beam by the quasi-Newton method.

Halim et al. [2003] suggested a criterion for the placement of collocated piezoelectric actuator-sensor pairs on a thin flexible plate using modal and spatial controllability measures. The reduction of control spillover effect by adding an extra spatial controllability constraint in the optimization procedure was considered. The spatial controllability is used to find the optimal placement of the collocated sensor-actuator pairs for effective average vibration reduction over the entire structure, while maintaining modal controllability and observability of the selected vibration modes. They found that the methodology for optimal actuator placement can be used for a collocated system without damaging the observability of the collocated sensors. They

experimentally validated the optimal placement done on a simply supported thin plate with a collocated piezoelectric sensor-actuator pair.

Quek at el. [2003] presented an optimal placement strategy of piezoelectric sensor actuator pairs for vibration control of laminated composite plate. They have maximized the active damping effect under a classical control frame work using the finite element approach. They have employed classical pattern search method to obtain the local optimum, where the two optimization performance indices based on modal and system controllability were studied. They have selected the start point for the pattern search method based on the maxima of integrated normal strains consistent with the size of the collocated piezoelectric patches used. The effectiveness of the strategy was illustrated by numerical simulation using a cantilevered and clamped composite square plate.

Smithmaitrie et al. [2004] evaluate the micro-control actions and distributed control effectiveness of segmented actuator patches laminated on hemispheric shells. They developed Mathematical models and governing equations of the hemispheric shells laminated with distributed actuator patches, followed by formulations of distributed control forces and microcontrol actions including circumferential membrane and bending control components. Their analysis indicates that the control forces and membrane/bending components are mode and location dependent, actuators placed near the free boundary contributes the most significant control actions, and the circumferential membrane control actions dominate the overall control effect.

Yue et al. [2008] focuses on analysis of microscopic control actions of segmented actuator patches laminated on the surface of a free paraboloidal membrane shell. They presented governing equations of the membrane shell system and modal control forces of distributed actuator patches and followed by the analysis of dominating micro-control actions based on various natural modes, actuator locations and geometrical parameters. Their simulation data reveal main factors significantly influencing active control behavior on smart free-floating paraboloidal membrane shell systems.

3.4 Experimental Work

Crawley et al. [1987] presented the analytical and experimental development of piezoelectric actuators as elements of intelligent structures i.e. structures with highly distributed actuators that are either bonded to an elastic substrate or embedded in a

laminated composite. These models lead to the ability to predict, a priori, the response of a structural member to a command voltage applied to the piezoelectric patch and give guidance as to the optimal location for the actuator placement. They performed a scaling analysis to demonstrate that the effectiveness of the piezoelectric actuators is independent of the size of the structure and to evaluate various piezoelectric materials based on their effectiveness in transmitting strain to the structure. They constructed three test specimens of cantilevered beams: an aluminum beam with surface bonded actuators, a glass/epoxy beam with embedded actuators and a graphite epoxy beam with embedded actuators. They used actuators to excite steady state resonant vibrations in the cantilever beams. The response of the specimen compared well with those predicted by the analytical models. Static tensile tests performed on glass/epoxy laminates indicated that the embedded actuators reduce the ultimate strength of the laminate structure by 20%, while not significantly affecting the global elastic modulus of the specimen.

Crawley et al. [1991] developed and experimentally verified the induced strain actuation of a plate. They derived equations relating the actuation strain created by induced strain actuators, to the strain induced in the actuator/substrate systems for isotropic and anisotropic plate. They also developed plate strain energy relations. They founded several exact solutions for simple actuator/substrate system and formulated a general procedure for solving the strain energy equation with Rayleigh-Ritz technique. They verified the accuracy of the basic induced strain actuator/substrate system models by using simple test articles and build cantilever plate test articles.

Han et al. [1997] applied active vibration control method both numerically and experimentally in order to reduce the vibration of light weight composite structure. They developed an analytical model of the laminated composite beam with piezoelectric sensors and actuators using classical laminated beam theory and Ritz method. They manufactured and tested smart composite beams and plates with surface bonded piezoelectric sensors and actuators. They designed and implemented a control system using linear quadratic Gaussian control algorithm and known classical control algorithms. They successfully controlled the first and second modes of a cantilever beam and simultaneous bending and twisting modes of a cantilever plate. They concluded that the linear quadratic Gaussian control algorithm shows robustness in noise and control efficiency compared with classical control methods.

Park et al. [2002] presented experimental investigations of the vibration testing of an inflated, thin-film torus using smart materials. They show that polyvinylidene fluoride (PVDF) patches and recently developed macro-fiber composite actuators may be used as sensors and actuators in identifying modal parameters. They suggested that the addition of actuators and PVDF sensors to the torus does not significantly interfere with the suspension modes of a free boundary condition, and can be considered an integral part of the inflated structure. Their results indicate the potential of using smart materials to measure and control the dynamic response of inflated structures.

Lee et al. [2003] presented an experimental study for the active vibration control of structures subjected to external excitations using piezoelectric sensors and actuators. They used a simply supported plate and a curved panel as the controlled structures in two experiments. They employed the independent model space control approach for the controller design. They also incorporated the time domain modal identification technique into the controller for real time update of the system parameter for increasing the adaptability. They have tested the adaptive effectiveness of the time domain modal identification technique by fixing an additional mass on the simply supported plate to change its structural properties.

Keir et al. [2004] analytically and experimentally investigated the active control of the structure-borne vibration transmission in resonant built up structures. They compared the control performance for both dependent and independent control force arrangements using feed forward active control. They used multiple actuator control forces and multiple error sensors to actively control the frequency response. They also presented the global response of coupled plate structure for active control at discrete resonance frequencies.

Mehrdad et al [2005] presented the manufacturing and testing of active composite panels (ACPs) with embedded piezoelectric sensors and actuators. They employed a cross ply type stacking sequence for the ACPs. The piezoceramic patches were embedded inside the composite laminate. The capacitance of the piezoelectric patches was measured before and after curing for quality control. The manufactured ACPs were trimmed and tested for their functionality. They developed a finite element model to verify the free expansion of the piezoceramic patches. The experimental results were compared with the finite element model and results showed good agreements. Finally

they successfully conducted vibration suppression as well as simultaneous vibration suppression and precision positioning tests using Hybrid adaptive control on manufactured ACP beams and demonstrated their functionality.

Qiu at el. [2006] describe the active vibration control of a plate using self sensing actuator and an adaptive control method. They stated that in a self sensing actuator, the same piezoelectric patch element functions as both sensor and actuator so that the total number of piezoelectric elements required can be reduced. They have proposed a method to balance the bridge circuits of self-sensing actuator and have confirmed its effectiveness by using an extra piezoelectric sensor. They established a control system including a self-sensing actuator and adaptive controller using a finite impulse response filter and the filtered-X LMS algorithm. They have experimentally validated their work and results showed that the bridge circuit was well balanced and the vibration of the plate was successfully reduced at multiple resonance frequencies.

Nagai et al. [2007] presented detailed experimental results and analytical results are on chaotic vibrations of a shallow cylindrical shell panel subjected to gravity and periodic excitation. First they find fundamental properties of the shell-panel, linear natural frequencies and characteristics of restoring force of the shell-panel. These results are compared with the relevant analytical results. Then, geometrical parameters of the shell panel are identified. Then they obtained nonlinear frequency responses of the shell panel by exciting the shell-panel with lateral periodic acceleration. In typical ranges of the exciting frequency, predominant chaotic responses are generated. Chaotic responses are integrated numerically by the Runge–Kutta–Gill method. The chaotic responses, which are obtained by the experiment and the analysis, are inspected with the Fourier spectra, the Poincare projections, the maximum Lyapunov exponents and the Lyapunov dimension. They found that the dominant chaotic responses of the shell-panel are generated from the responses of the sub-harmonic resonance of 12 order and of the ultra-sub-harmonic resonance of 23 order.

Kurpa et al. [2007] conducted experiments on an aluminum panel with complex shape of the boundary in order to identify the nonlinear response of the fundamental mode; these experimental results have been compared to numerical results.

Barrault et al. [2008] combined the frequency bandwidth to be controlled, the accuracy of the structural modelling, the robustness of the controller, and the extent to

which the disturbance can be quantified to produce a robust, fixed bandwidth controller for which the lower frequency limit for control can be any frequencies larger than 0 Hz. They showed how Subspace Model identification can be used to obtain the system dynamics through experiment. After combining these theories they showed experimentally how to achieve global vibration attenuation for the system.

Zhang et al.[2008] studied active vibration control of a cylindrical shell partially covered by a laminated PVDF actuator and carried out an experiment to actively control vibration of a clamped–free cylindrical shell using an LPA with different layer numbers. They showed that the control forces of the actuator can be significantly enhanced by increasing the PVDF layer number while keeping the driving voltage unchanged and as a result they showed the modal vibrations of the shell are suppressed quite well under a relatively low control voltage (40 V) with a five-layer LPA whose area is only 0.21% of that of the shell.

Chapter 4

BASIC EQUATIONS AND FORMULATIONS

4.1 Definition of coordinate systems

The degenerated shell element is obtained from the 3D solid element through the degeneration process [Balamurugan, (2008)]. The degeneration process from the 3D solid element to shell element is based on Mindlin– Reissner kinematical assumptions:

- The normal to mid surface of shell remain straight but need not necessarily remain normal after deformation. Therefore, transverse shear strain is included and thus the degenerated shell element is a mindlin element.
- Strain energy associated with the normal strain perpendicular to the local mid surface is neglected. i.e., the transverse normal components of stress are ignored in the development. The shell element admits arbitrarily large displacement and rotation but the strain are assumed to be small since the shell thickness is assumed to remain unchanged and the normal is not allowed to distort.
- The rotation about the normal to the midsurface is neglected.
- All layers are perfectly bonded.
- The piezoelectric patches are much thinner than the host structure, and are perfectly bonded to the surface of the structure. The effects of the bonding material on the properties of the whole structure are neglected.

The result of the degeneration process is that the displacement of any point in the volume of the element can be described in terms of six global degrees of freedom of the appropriate mid-surface point, three translations and three rotations. Three different coordinate systems are used in the formulation of the element: the global coordinate system (x, y, z), natural coordinate system (ξ, η, ζ) and local-running coordinate system (x', y', z') and they are shown in figure 4.1.

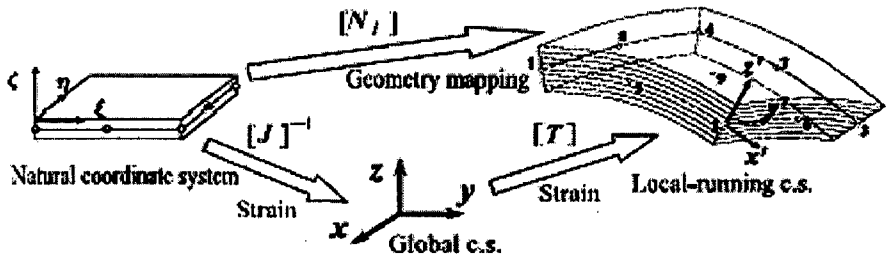

Figure 4.1: Coordinate system for general shell element.

A nine-noded 3D shell element geometry is shown in figure 4.1. The external surfaces of the shell may be flat or curved, sections across the thickness are generated by straight lines and pairs of points on the top and bottom surfaces are prescribed by the shape of the element. The global coordinates of any arbitrary point in the above shell domain can be expressed using the nodal coordinates and isoparametric shape functions as

$$\begin{Bmatrix} x \\ y \\ z \end{Bmatrix} = \sum_{i=1}^{9} N_i(\xi,\eta)\frac{1+\xi}{2}\begin{Bmatrix} x_i \\ y_i \\ z_i \end{Bmatrix}_{top} + \sum_{i=1}^{9} N_i(\xi,\eta)\frac{1-\xi}{2}\begin{Bmatrix} x_i \\ y_i \\ z_i \end{Bmatrix}_{bottom} \tag{4.1}$$

where *Ni* (ξ, η) is the quadratic shape function at node i . Equation (4.1) may be conveniently written in the form specified by the vector connecting the upper and lower points of the shell and the mid-surface coordinates as given below:

$$\begin{Bmatrix} x \\ y \\ z \end{Bmatrix} = \sum_{i=1}^{9} N_i(\xi,\eta)\begin{Bmatrix} x_i \\ y_i \\ z_i \end{Bmatrix}_{mid} + \sum_{i=1}^{9} N_i(\xi,\eta)\xi\frac{h_i}{2}\begin{Bmatrix} l_{3i} \\ m_{3i} \\ n_{3i} \end{Bmatrix} \tag{4.2}$$

with

$$e_{3i} = \begin{Bmatrix} l_{3i} \\ m_{3i} \\ n_{3i} \end{Bmatrix} = \frac{1}{h_i}\left\{ \begin{Bmatrix} x_i \\ y_i \\ z_i \end{Bmatrix}_{top} - \begin{Bmatrix} x_i \\ y_i \\ z_i \end{Bmatrix}_{bottom} \right\} \tag{4.3}$$

where e_{3i} is the unit vector normal to the mid-surface and h_i is the nodal thickness of the element.

4.2 Displacement equation

Displacements of the shell element at any point are described with respect to the global coordinate system. The nodal displacements throughout the element domain are uniquely defined by the three translation components of the mid-surface nodal displacements in global directions, u_i , v_i and w_i , and two rotations θ_{xi} and θ_{yi} of the nodal vector e_{3i} about the orthogonal direction normal to it (i.e. about the local tangential axes x' and y' respectively). Let e_{1i} and e_{2i} be two orthogonal directions tangential to the plane of the flat shell element. These vectors can be described by

$$\begin{Bmatrix} e_{1i} \\ e_{2i} \\ e_{3i} \end{Bmatrix} = \begin{pmatrix} l_{1i} & m_{1i} & n_{1i} \\ l_{2i} & m_{2i} & n_{2i} \\ l_{3i} & m_{3i} & n_{3i} \end{pmatrix} \tag{4.4}$$

where l_{1i} , l_{2i} , l_{3i} ,m_{1i} ,m_{2i} ,m_{3i} , n_{1i} , n_{2i} , n_{3i} are the corresponding direction cosines between the global (x, y, z) axes system and local-running (x', y' , z') axes system at every node. They can be easily evaluated from the Jacobian of the transformation between the global and isoparametric coordinate systems (ξ, η, ζ). The global displacements at any point in the element domain can be written in terms of nodal displacements as

$$\begin{Bmatrix} u \\ v \\ w \end{Bmatrix} = \sum_{i=1}^{9} N_i \begin{Bmatrix} u_i \\ v_i \\ w_i \end{Bmatrix} + \sum_{i=1}^{9} N_i \xi \frac{h_i}{2} \begin{pmatrix} l_{1i} & l_{2i} \\ m_{1i} & m_{2i} \\ n_{1i} & n_{2i} \end{pmatrix} \begin{Bmatrix} \theta_{xi} \\ \theta_{yi} \end{Bmatrix} \tag{4.5}$$

where $\{q\}_e = \{u_i, v_i, w_i, \theta_{xi}, \theta_{yi}\}^T$ are the nodal displacement vector.

4.3 Constitutive equations of piezoelectric materials

The linear piezoelastic constitutive equation of piezoelastic continuum subjected to displacement and electrical fields are governed by the converse and direct piezoelectric effect. The converse piezoelectric effect equations are given by

$$\begin{Bmatrix} \begin{Bmatrix} \sigma_{xx} \\ \sigma_{yy} \\ \tau_{xy} \end{Bmatrix} \\ \begin{Bmatrix} \tau_{xz} \\ \tau_{yz} \end{Bmatrix} \end{Bmatrix} = \begin{pmatrix} \begin{pmatrix} Q11 & Q12 & 0 \\ Q21 & Q22 & 0 \\ 0 & 0 & Q66 \end{pmatrix} & \begin{pmatrix} 0 & 0 \\ 0 & 0 \\ 0 & 0 \end{pmatrix} \\ \begin{pmatrix} 0 & 0 & 0 \\ 0 & 0 & 0 \end{pmatrix} & \begin{pmatrix} Q44 & Q45 \\ Q54 & Q55 \end{pmatrix} \end{pmatrix}$$

$$\text{X} \quad \begin{Bmatrix} \begin{Bmatrix} \varepsilon_{xx} \\ \varepsilon_{yy} \\ \gamma_{xy} \end{Bmatrix} \\ \begin{Bmatrix} \gamma_{xz} \\ \gamma_{yz} \end{Bmatrix} \end{Bmatrix} - \begin{pmatrix} \begin{pmatrix} 0 & 0 & e31 \\ 0 & 0 & e32 \\ 0 & 0 & e36 \end{pmatrix} \\ \begin{pmatrix} e14 & e24 & 0 \\ e15 & e25 & 0 \end{pmatrix} \end{pmatrix} \begin{Bmatrix} E_x \\ E_y \\ E_z \end{Bmatrix} \tag{4.6a}$$

while the direct piezoelectric equations are given by

$$\begin{Bmatrix} D_x \\ D_x \\ D_x \end{Bmatrix} = \begin{pmatrix} 0 & 0 & 0 \\ 0 & 0 & 0 \\ e31 & e32 & e36 \end{pmatrix} \begin{Bmatrix} \varepsilon_{xx} \\ \varepsilon_{yy} \\ \varepsilon_{zz} \end{Bmatrix} + \begin{pmatrix} e14 & e15 \\ e24 & e25 \\ 0 & 0 \end{pmatrix} \begin{Bmatrix} \gamma_{xz} \\ \gamma_{yz} \end{Bmatrix} + \begin{pmatrix} \varepsilon 11 & \varepsilon 12 & 0 \\ \varepsilon 21 & \varepsilon 22 & 0 \\ 0 & 0 & \varepsilon 33 \end{pmatrix} + \begin{Bmatrix} E_x \\ E_y \\ E_z \end{Bmatrix} \tag{4.6b}$$

These equations can be represented in a simplified form as

$$\begin{Bmatrix} \{\sigma_p\} \\ \{\tau_t\} \end{Bmatrix} = \begin{pmatrix} [Q_p] & [0] \\ [0] & [Q_t] \end{pmatrix} \begin{Bmatrix} \{\varepsilon_p\} \\ \{\gamma_t\} \end{Bmatrix} - \begin{pmatrix} [e_p]^T \\ [e_t]^T \end{pmatrix} \{E\}$$

$$\text{and} \quad \{D\} = \begin{bmatrix} e_p & e_t \end{bmatrix} \begin{Bmatrix} \varepsilon_p \\ \gamma_t \end{Bmatrix} + [\mathfrak{d}]\{E\} \tag{4.6c}$$

where $\{\sigma_p\}$ and $\{\tau_t\}$ are the in-plane stress components (in Nm^{-2}) and transverse shear stress components (in $N\ m^{-2}$). $\{\varepsilon_p\}$ and $\{\gamma_t\}$ are the corresponding strains. $[Q_p]$ and $[Q_t]$ are the plane stress reduced elasticity matrix (in $N\ m^{-2}$) and transverse shear elasticity matrix (in $N\ m^{-2}$). $[e_p]$ and $[e_t]$ are piezoelectric stress constants (in $C\ m^{-2}$). $[\mathfrak{d}]$ are permittivity constants (in $F\ m^{-1}$). $\{E\}$ and $\{D\}$ are the electric field (in $V\ m^{-1}$) and the electrical displacement (in $C\ m^{-2}$), respectively.

4.4 Strain displacement relations

The strain components with respect to the global coordinates can be expressed from the displacements as

$$\{\varepsilon\} = \begin{Bmatrix} \varepsilon_{xx} \\ \varepsilon_{yy} \\ \varepsilon_{zz} \\ \gamma_{xy} \\ \gamma_{yz} \\ \gamma_{xz} \end{Bmatrix} = \begin{Bmatrix} u,x \\ v,y \\ w,z \\ u,y+v,x \\ v,z+w,y \\ u,z+w,x \end{Bmatrix} = [B_u]\{q\}_e$$

$$= \left[\left[B_{u1} \right], \left[B_{u2} \right] \ldots\ldots\ldots \left[B_{u9} \right] \right] \begin{Bmatrix} q_1 \\ q_2 \\ \vdots \\ q_9 \end{Bmatrix} \tag{4.7}$$

where the matrix $[B_u]$ is called the strain displacement matrix and $\{q\}_e$ is the nodal displacement vector for an element. Here $[B_{ui}]$ and $\{q_i\}$ are given by

$$[B_{ui}] = \begin{bmatrix} a_i & 0 & 0 & d_i l_{1i} & d_i l_{2i} \\ 0 & b_i & 0 & e_i m_{1i} & e_i m_{2i} \\ 0 & 0 & c_i & g_i n_{1i} & g_i n_{2i} \\ b_i & a_i & 0 & e_i l_{1i} + d_i m_{1i} & e_i l_{2i} + d_i m_{2i} \\ 0 & c_i & b_i & g_i m_{1i} + e_i n_{1i} & g_i m_{2i} + e_i n_{2i} \\ 0 & 0 & a_i & d_i n_{1i} + g_i l_{1i} & d_i n_{2i} + g_i l_{2i} \end{bmatrix} \tag{4.8}$$

$$\{q_i\} = \begin{Bmatrix} u_i \\ v_i \\ w_i \\ \theta_{xi} \\ \theta_{yi} \end{Bmatrix} \tag{4.9}$$

where i = 1–9 for a nine-noded shell element. The matrix coefficients are given by

$$\begin{Bmatrix} a_i \\ b_i \\ c_i \end{Bmatrix} = \begin{bmatrix} J'11 & J'12 \\ J'21 & J'22 \\ J'31 & J'32 \end{bmatrix} \begin{Bmatrix} N_{i,\xi} \\ N_{i,\eta} \end{Bmatrix}$$

$$\begin{Bmatrix} d_i \\ e_i \\ g_i \end{Bmatrix} = \frac{h_i}{2}\xi \begin{Bmatrix} a_i \\ b_i \\ c_i \end{Bmatrix} + \begin{Bmatrix} J'13 \\ J'23 \\ J'33 \end{Bmatrix} N_i \tag{4.10}$$

where J is the Jacobian and J' is the inverse Jacobian of the transformation between global Cartesian coordinates and the local isoparametric coordinates and are given by

$$J = \begin{bmatrix} x,\xi & y,\xi & z,\xi \\ x,\eta & y,\eta & z,\eta \\ x,\zeta & y,\zeta & z,\zeta \end{bmatrix} \tag{4.11}$$

$$J^{-1} = J' = \begin{bmatrix} \xi,x & \eta,x & \zeta,x \\ \xi,y & \eta,y & \zeta,y \\ \xi,z & \eta,z & \zeta,z \end{bmatrix} \tag{4.12}$$

The material properties are available in the local-running coordinates and hence the strains with respect to the global coordinates $\{\varepsilon\}$ defined earlier need to be transformed into the strains with respect to the local running coordinates (x', y', z'). The local strains $\{\varepsilon'\}$ are related to the global strains $\{\varepsilon\}$ as

$$\{\varepsilon'\} = \begin{Bmatrix} \{\varepsilon_p'\} \\ \{\gamma_t'\} \end{Bmatrix} = \begin{Bmatrix} \varepsilon_{x'x'} \\ \varepsilon_{y'y'} \\ \gamma_{x'y'} \\ \gamma_{y'z'} \\ \gamma_{z'x'} \end{Bmatrix} = \begin{Bmatrix} \dfrac{\partial u}{\partial x'} \\ \dfrac{\partial v}{\partial y'} \\ \dfrac{\partial u}{\partial y'} + \dfrac{\partial v}{\partial x'} \\ \dfrac{\partial v}{\partial z'} + \dfrac{\partial w}{\partial y'} \\ \dfrac{\partial w}{\partial x'} + \dfrac{\partial u}{\partial z'} \end{Bmatrix} = [T_\varepsilon] = \begin{Bmatrix} \varepsilon_{xx} \\ \varepsilon_{yy} \\ \gamma_{xy} \\ \gamma_{yz} \\ \gamma_{zx} \end{Bmatrix}$$

$$= [T\varepsilon]\{\varepsilon\} \tag{4.13}$$

where $[T_\varepsilon]$ is a (5 × 6) strain transformation matrix given by

$$[T_\varepsilon] = \begin{bmatrix} l_1^2 & m_1^2 & n_1^2 & l_1 m_1 & m_1 n_1 & n_1 l_1 \\ l_2^2 & m_2^2 & n_2^2 & l_2 m_2 & m_2 n_2 & n_2 l_2 \\ 2l_1 l_2 & 2m_1 m_2 & 2n_1 n_2 & l_1 m_2 + l_2 m_1 & m_1 n_2 + m_2 n_1 & n_1 l_2 + n_2 l_1 \\ 2l_2 l_3 & 2m_2 m_3 & 2n_2 n_3 & l_2 m_3 + l_3 m_2 & m_2 n_3 + m_3 n_2 & n_2 l_3 + n_3 l_2 \\ 2l_3 l_1 & 2m_3 m_1 & 2n_3 n_1 & l_3 m_1 + l_1 m_3 & m_3 n_1 + m_1 n_3 & n_3 l_1 + n_1 l_3 \end{bmatrix} \tag{4.14}$$

where, l_1, l_2, l_3,m_1,m_2,m_3, n_1, n_2, n_3 are the corresponding direction cosines between the global coordinate system and local-running coordinate system. These can be evaluated conveniently from the Jacobian (equation (4.11)) of the transformation between the global coordinate system and the isoparametric coordinate system. For a general point in the shell element, the direction cosines are given by

$$\begin{aligned} e_1 &= \{l_1 \quad m_1 \quad n_1\}^T = (J_1) \\ e3 &= \{l_3 \quad m_3 \quad n_3\}^T = (J_1 \times J_2) \\ e2 &= \{l_2 \quad m_2 \quad n_2\}^T = (e_3 \times e_1) \end{aligned} \tag{4.15}$$

where e_1, e_2 and e_3 are the unit vectors along the local-running coordinates (x', y', z'). J_i is the i th column of the Jacobian matrix and '×' represents the cross product of vectors. Also 'norm' indicates the norm of the vector. In terms of strain displacement relations equation (4.13) can be written as

$$\{\varepsilon'\} = [B'_u]\{q_e\} = [T][B_u]\{q_e\} \tag{4.16}$$

Hence the strain displacement matrix corresponding to the local-running coordinates $[B'_u]$ is given by

$$[B'_u] = [T_\varepsilon][B] \tag{4.17}$$

4.5 Dynamic Equations

When one piezoelectric layer acts as sensor and actuator, the structure is termed as a smart structure. At any instant sensor senses the deformation or deflection and a proportional voltage is fed to the controller, which generates controlling voltage for the actuator layer. In this case total voltage can be partitioned into sensor voltage and actuator voltage. So the governing equation of motion for an element using the Hamilton principle can be given by

$$[M_{uu}]_e\{\ddot{q}\}_e+[C_{uu}]_e\{\dot{q}\}_e+[K_{uu}]_e\{q\}_e+\left[K_{u\phi}\right]_e\left\{\hat{\phi}\right\}_e=\left\{F_q\right\}_e \tag{4.18a}$$

$$\left[K_{\phi u}\right]_e\{q\}_e+\left[K_{\phi\phi}\right]_e\left\{\hat{\phi}\right\}_e=\left\{F_\phi\right\}_e \tag{4.18b}$$

where. $[M_{uu}]_e$, $[K_{uu}]_e$, $[K_{u\varphi}]_e$, $\{F_q\}_e$, $[K_{\varphi\varphi}]_e$ and $\{F_\varphi\}_e$ are the element mass matrix, stiffness matrix, electromechanical coupling stiffness matrix, mechanical load, dielectric stiffness matrix and force vector, respectively, while $[C_{uu}]_e$ is the structural damping matrix Equations (4.18a) and (4.18b) can be combined as

$$[M_{uu}]_e\{\ddot{q}\}_e+[C_{uu}]_e\{\dot{q}\}_e+\left[[K_{uu}]_e-\left[K_{u\phi}\right]_e\left[K_{\phi\phi}\right]_e^{-1}\times\left[K_{u\phi}\right]_e\right]\{q\}_e$$

$$=\left\{F_q\right\}_e-\left[K_{u\phi}\right]_e\left[K_{\phi\phi}\right]_e^{-1}\left\{F_\phi\right\}_e \tag{4.19}$$

Applying equation (4.18b) to sensors with zero external applied charge, the sensed voltage is

$$\left\{\hat{\phi}_S\right\}_e=-\left[K_{\phi\phi}\right]_{se}^{-1}\left[K_{u\phi}\right]_{se}\left\{q_S\right\}_e \tag{4.20}$$

The global equations of motion, obtained by assembling elemental equations, are given by

$$[M_{uu}]\{\ddot{q}\}+[C_{uu}]\{\dot{q}\}+\left[[K_{uu}]-\left[K_{u\phi}\right]\left[K_{\phi\phi}\right]^{-1}\left[K_{\phi u}\right]\right]\{q\}$$

$$=\left\{F_q\right\}-\left[K_{u\phi}\right]\left\{\hat{\phi}_a\right\} \tag{4.21}$$

where $\{\hat{\phi}_a\}$ is the actuator voltage.

4.6 The Sensor Equation

Since no external electric field is applied to the sensor layer and as the charge is collected only in the thickness direction, only the electric displacement D_z is of interest. D_z can be expressed as:

$$D_z = e_{31}\varepsilon_x + e_{32}\varepsilon_y + e_{36}\gamma_{xy} = [e_3]\{\varepsilon\} \tag{4.22}$$

where

$$[e_3] = [e_{31} \quad e_{32} \quad e_{36}] \tag{4.23}$$

The total charge developed on the sensor surface is the spatial summation of all the point charges on sensor layer. Hence the closed circuit charge measured through the electrodes of the sensor patch can be expressed as:

$$q(t) = \sum_{j=1}^{N_s} \left[\frac{1}{2} \int_{-1}^{1} \int_{-1}^{1} [e_3](2[A] - (z_k + z_{k+1})[C])|J| d\xi d\eta \right] \left\{ u_j^e \right\}, \tag{4.24}$$

If sensor is bonded at the upper surface of the semi-circular cylindrical shell,

$$z_{k+1} = \left(\frac{t}{2} + t_p \right), \quad z_k = \frac{t}{2} \tag{4.25}$$

and if sensor is bonded to the lower surface of the semi-circular cylindrical shell,

$$z_{k+1} = -\frac{t}{2}, \quad z_k = -\left(\frac{t}{2} + t_p \right) \tag{4.26}$$

4.7 The Control Laws

The block diagram of the vibration control system is shown in the figure 4.2. It is single input single output feedback control system. The feedback signal is generated by

the piezoelectric sensor. The signal is then amplified with gain and applied to the piezoelectric actuator.

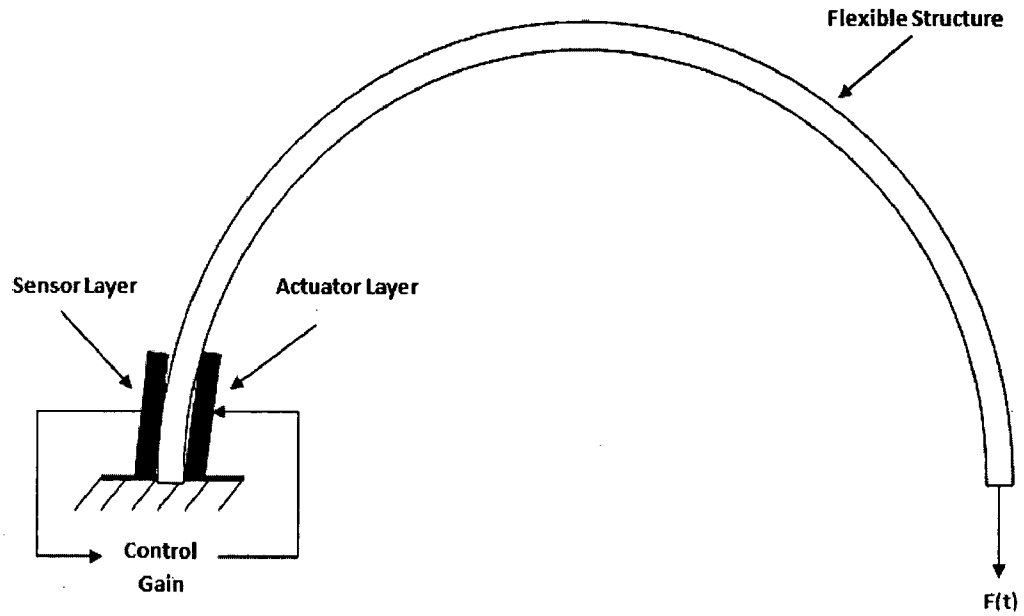

Figure 4.2: A flexible structure with actuator and sensor.

Depending upon the type of the signal conditioning, the actuation action in proportional control is function of position like quantities

(1) Proportional control method: In proportional control method, the feedback voltage V^e is obtained by multiplying sensing voltage V_s^e with gain G. Gain value for the vibration suppression is chosen arbitrarily, therefore the control equation is written in given form.

$$V^e = GV_s^e \tag{4.27}$$

4.8 Boundary conditions

Semi-circular cylindrical cantilevered shell

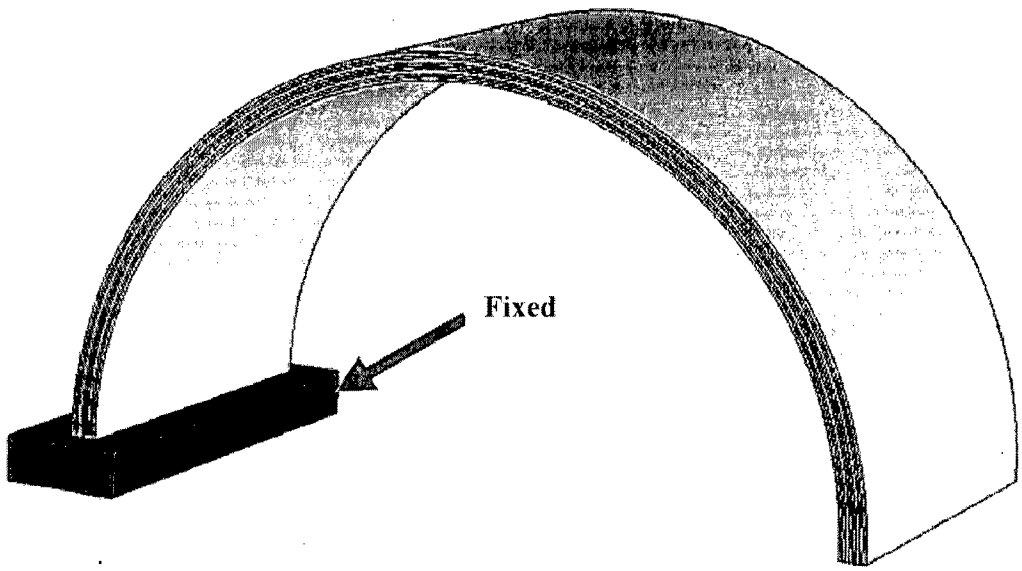

Figure 4.3: Boundary condition for semi circular cylindrical cantilevered shell.

Chapter 5

EXPERIMENTATION

The experimental setup fabricated for the present work is described in this chapter. Detailed specification of devices used in the experimentation is given. This chapter also includes the procedure and method used for the setup.

5.1 Experimentation

5.1.1 Objectives:

(1) To monitor the real time vibration signal of semi-circular cylindrical shells specimens.

(2) To record the signal file and to find the response of the semi-circular cylindrical shell using sensor voltage.

(3) To implement active vibration control using closed loop proportional control.

(4) To know the performance of proportional controller with semi circular cylindrical shell, when the shell is vibrating in I^{st} mode.

5.1.2 Equipments:

Following equipments are used in the experimental work.

(1) Semi-circular cylindrical shell specimen(R=200mm, W=210mm & T= 0.75mm).

(2) Vibration control unit (Piezo sensing and actuation system).

(3) Piezoelectric sensor and piezoelectric actuator (PZT patches).

(4) USB based Data acquisition card (NI make).

(5) Computer with LABView software version 8.0

(6) Connections BNC connector cables.

(7) Power supply 240V, 50 Hz

Specification of all the equipments are given in the table 5.1 to table 5.4

Table 5.1: Material properties of semi-circular cylindrical shell.

Physical Properties	**Metric**
Density	2.83 g/cc
Ultimate Tensile Strength	607 MPa
Tensile Yield Strength	538 MPa
Modulus of Elasticity	71.7 GPa
Compressive Yield Strength	530 MPa
Notched Tensile Strength	386 MPa
Ultimate Bearing Strength	1089 MPa
Bearing Yield Strength	807 MPa
Poisson's Ratio	0.33
Fatigue Strength	150 MPa
Shear Modulus	27 GPa
Shear Strength	360 MPa
Electrical Resistivity	5.49e-006 ohm-cm
Specific Heat Capacity	0.856 J/g-°C
Thermal Conductivity	125 W/m-K

Table 5.2: Specifications of the vibration control unit by Spranktronics Inc.

Piezo sensing system

Sensor	Piezo electric crystal
Output	Sine/random
No of channels	2
Frequency range	10- 2000 Hz
Maximum input voltage	10 volt (RMS)
Maximum output voltage	200 volt (RMS)
Input / output connection	PT 10 terminals / B & C connectors
Input power	230 V, 50 Hz AC

Piezo actuation system

Actuator	Piezo electric crystal
Output	Sine/random
No of channels	2
Frequency range	10- 2000 Hz
Maximum output voltage	200 volt (RMS) (adjustable gain)
Input / output connection	PT 10 terminals / B & C connectors
Input power	230 V, 50 Hz AC

Table 5.3: Properties of the piezoelectric sensor and actuator (PZT patches) by Sparkler Ceramics pvt. Ltd.

Property name	
Material	Lead zirconate titanate.
Dimension (mm)	30 X 30 X 0.5
Young's Modulus (N/m^2)	63E09
Density (Kg/m^3)	7600
Dielectric constant (d_{31}) (m/V)	254e-12
Stress constant (g_{31})(Vm/N)	9E-3

Table 5.4: USB based Data acquisition NI USB-6009card by National Instruments Inc.

Analog Input	
Converter type	Successive approximation
Analog inputs	8 single-ended
Input resolution	14 bits differential 13 bits single-ended
Max sampling rate (aggregate)	48 kS/s
Timing resolution	41.67 ns (24 MHz timebase)
Timing accuracy	100 ppm of actual sample rate
Input range	±10 V
Input impedance	144 kΩ
Overvoltage protection	±35

Analog Output	
Analog outputs	2
Output resolution	12 bits
Maximum update rate	150 Hz, software-timed
Output range	0 to +5 V
Output impedance	50 Ω
Output current drive	5 mA
Short circuit current	50 mA
Absolute accuracy (no load)	7 mV typical,36.4 mV maximum at full scale
Power Requirements USB 4.10 to 5.25 VDC USB suspend	 80 mA typical, 500 mA max 300 µA typical, 500 µA max
Physical Characteristics	
Dimensions Without connectors With connectors	 6.35 cm × 8.51 cm × 2.31 cm 8.18 cm × 8.51 cm × 2.31 cm
I/O connectors	USB series B receptacle, (2) 16 position terminal block plug headers
Weight With connectors Without connectors	 84 g (3 oz) 54 g (1.9 oz)
Screw-terminal wiring	16 to 28 AWG

5.2 Experimental setup

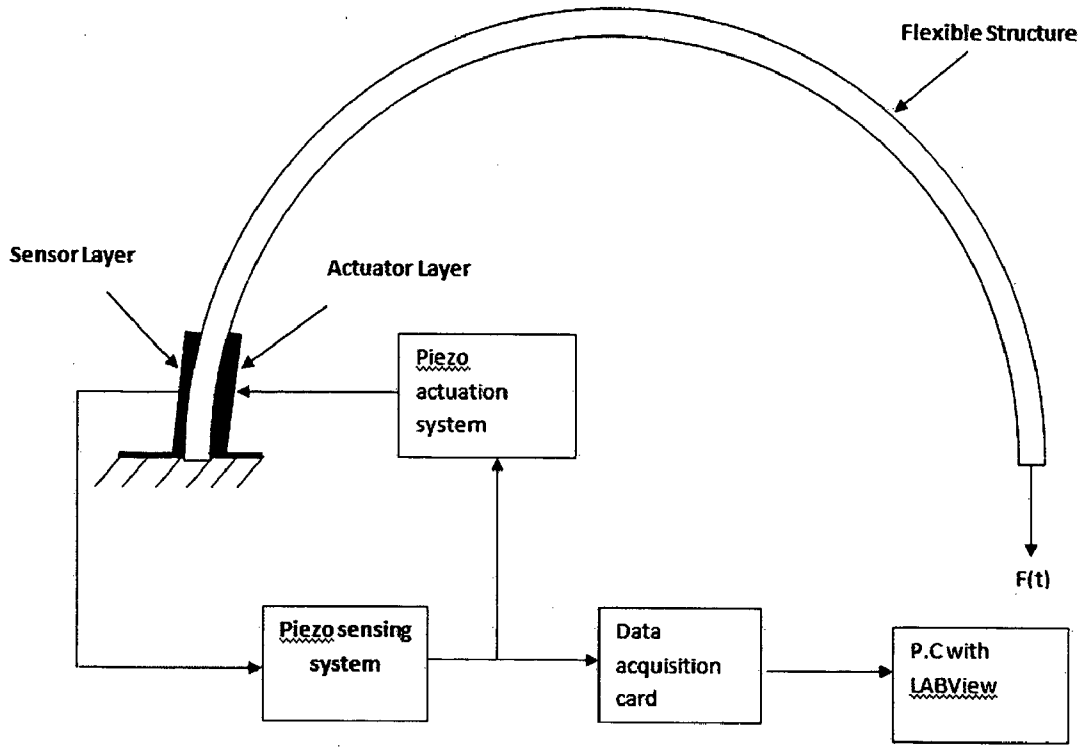

Figure 5.1(a): Block diagram of the experimental setup.

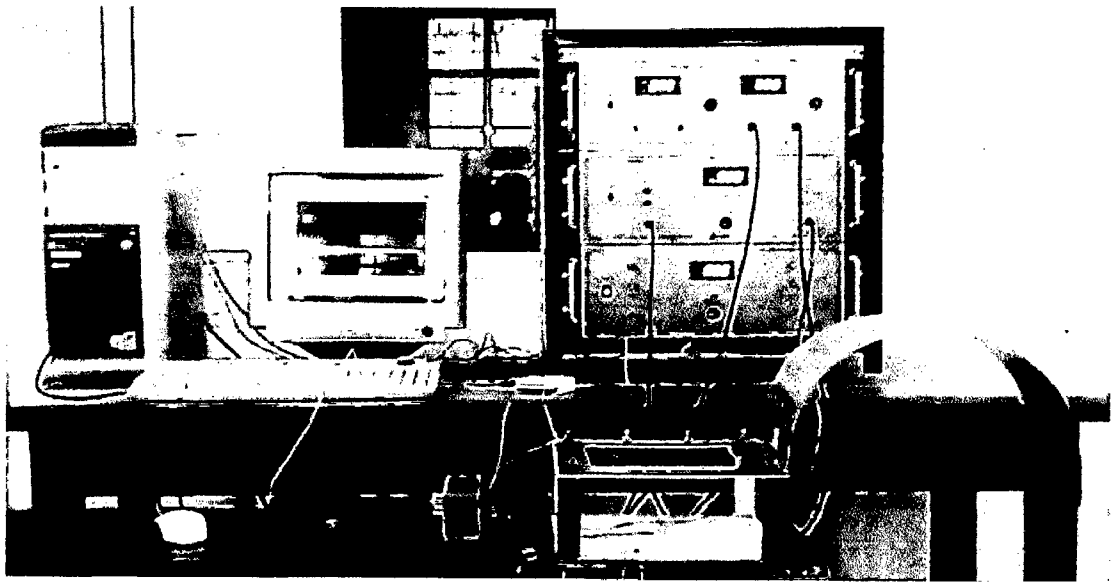

Figure 5.1 (b): Experimental setup of the active vibration control.

Figure 5.1(a) shows the schematic block diagram and Figure 5.1 (b) shows the experimental setup of the active vibration control. It is seen from the above diagram that

PZT patch, piezo sensing and actuation system form a closed control loop. Functions of each of the above components are explained in the following sub section.

5.2.1 PZT patch

Smart material used in the experiment is PZT patch made by the Sparkler Ceramics pvt ltd with detail specification given in the table 5.3. Two PZT patches are used for the vibration suppression of each semi-circular cylindrical shell. For the cantilever semi-circular cylindrical shell, one PZT is mounted near the clamped end at the middle of the lateral direction and other PZT is mounted at the same location but on the other side of the semi-circular cylindrical shell in a symmetric fashion. One PZT patch acts as sensor and other acts as the actuator. Patch is bonded to the structure using epoxy as shown in the figure 5.2. When the semi-circular cylindrical shell is excited by impulse, it starts vibrating and the sensor when deformed mechanically develops the voltage across it terminals.

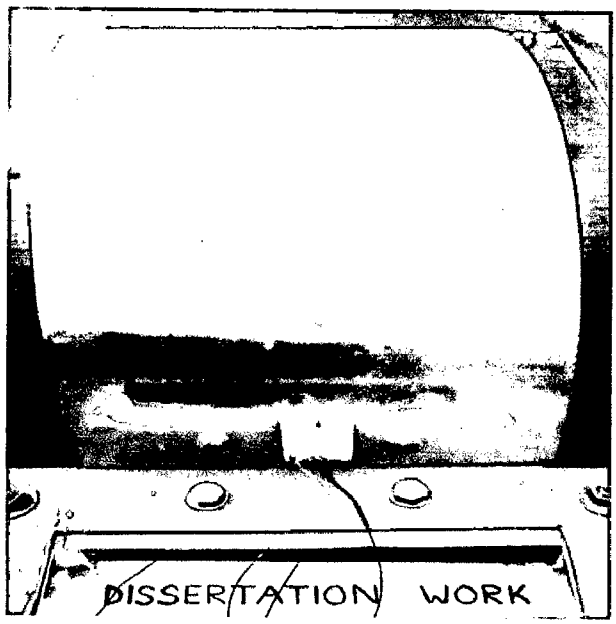

Figure 5.2: Location of the PZT patch.

5.2.2 USB based data acquisition

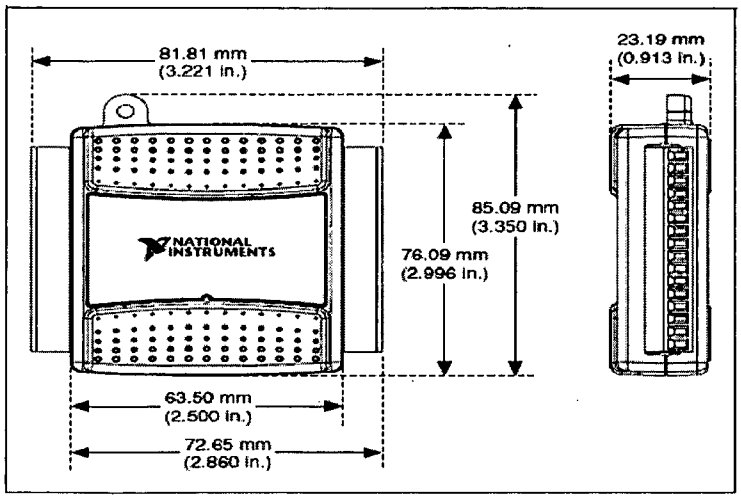

Figure 5.3: NI make DAQ card – NI 6009.

As shown in the figure 5.3, data acquisition system is a National Instrument Inc. product. This card may be used for measuring and recording of various parameters like displacement, voltage, velocity, acceleration, strain, temperature etc. in a machine, equipments or any other mechanical components. PC based DAQ normally finds application in storing real time signal. It is able to store the signal parameter so that later on it can be easily used for further analysis. Various internal devices are used for signal measurement and conversion. One of the most useful devices is the analog to the digital and digital to analog converter. Multiplexer is used to combine several input signals into a vector from for the I/O port. Counters and timers are used to control the signal time and also keep the data in the buffer for the required amount of time. Counter clock runs with CPU clock and is used to synchronize all elements.

In this experimentation, National instrument make USB based DAQ is used. Semi-circular cylindrical shell is excited at tip with unknown impulse and PZT sensor bonded to of the semi-circular cylindrical shell sends the sensed signal. This voltage is amplified by the piezo sensing system and is given to the NI card and piezo actuator system. It is able to sense the voltage generated by the PZT sensor mounted on the semi-circular cylindrical shell surface. PZT sensor is connected to the DAQ card through signal sensing device. The sensed voltage is scanned and stored in the computer using LABView software version 8.0. The stored file can be used for further post processing. The input port of the N.I card is adjustable & is adjusted with the help of DAQ assistance

in LABview. Through DAQ assistance connection to the DAQ card can be identified. The connection are shown in figure 5.4

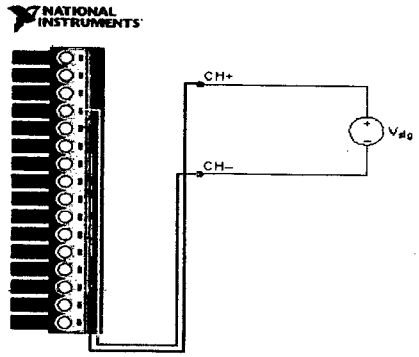

Figure 5.4: Connection of DAQ card.

5.2.3 Piezo sensing and actuation system

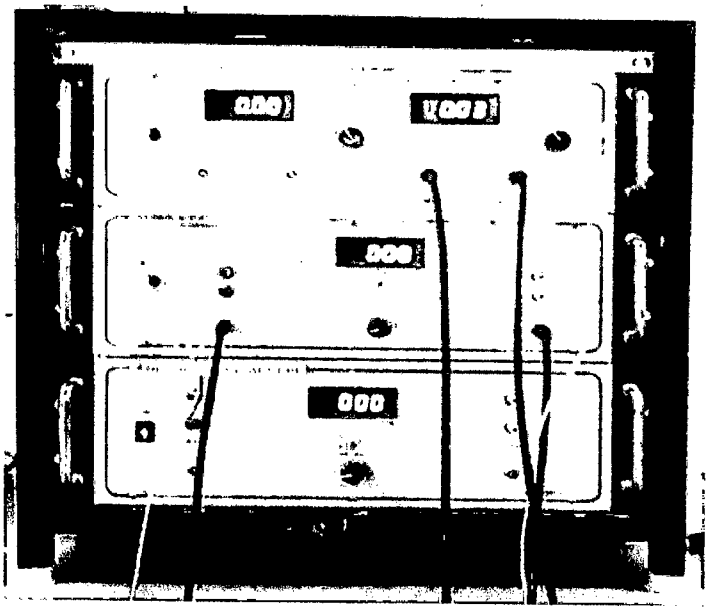

Figure 5.5: Piezo sensing and Piezo actuation system.

Piezo sensing and actuation system shown in figure 5.5 was used in the experiment for sensing the strain generated in the PZT patch and for amplifying the signal so that it can be used for further processing. This system has two channel sensing and two channel actuation capability. Output of the PZT sensor is connected to the sensing system using BNC cable and output of this sensing device is connected to the NI card and also connected to the actuation system. Piezo actuation system is a voltage

amplifier which amplifies the voltage sensed by the sensing system so that it can actuate the PZT for vibration suppression.

This system has the capability that is operate in both in and out of phase of the signal. First the signal is inverted and amplified by the system and then it is supplied to the PZT actuator. If the sensed signal is in phase then output signal can be made out of phase for the suppression of the vibration of the structure. The output gain may be adjusted by the knob on the actuation and sensing system. The vibration control can be made more effective by increasing the gain value of the piezo actuation system.

5.2.4 Computer with LABView software

DAQ card is connected to the computer using USB data cable with USB port of the PC. LabVIEW programs are called virtual instruments, or VIs, because their appearance and operation imitate physical instruments, such as oscilloscopes and multimeters. LabVIEW contains a comprehensive set of tools for acquiring, analyzing, displaying, and storing data. LabVIEW can be used to build a user interface, or front panel, with controls and indicators. Controls are in form of knobs, push buttons, dials, and other input mechanisms. Indicators are graphs, LEDs, and other output displays. After building the user interface, an additional code may be added using VIs and structures to control the front panel objects. The block diagram contains this code.

One VI is developed in the software that scans the data from the NI DAQ card. The data can be seen in the real time mode and through FFT it is possible to plot the frequency plot of the time base data. Figure 5.6 (a) and 5.6 (b) show the block diagram of the program and front panel of the VI. In the block diagram, the voltage signal is scanned using the DAQ assistant block and various parameter can be setup as shown in the figure 5.7. It is also possible to change the sampling rate and frequency rate. As shown in the block diagram, the wire is connected to graph indicator block where it is possible to see the real time signal of the sensor from the PZT. Band pass filter block is fixed between the graph indicator and DAQ assistant and between the FFT block and DAQ assistant so that it removes the high frequency component from the signal. FFT block is used here for finding the natural frequency of the signal so that it can be compared to the modal frequency and the theoretical frequency. Both time domain file and FFT file can be stored on the hard disc of the PC using file to measurement block as

shown in the block diagram Front panel of the VI shows only two graphs, one for the time domain signal and other for the frequency domain signal.

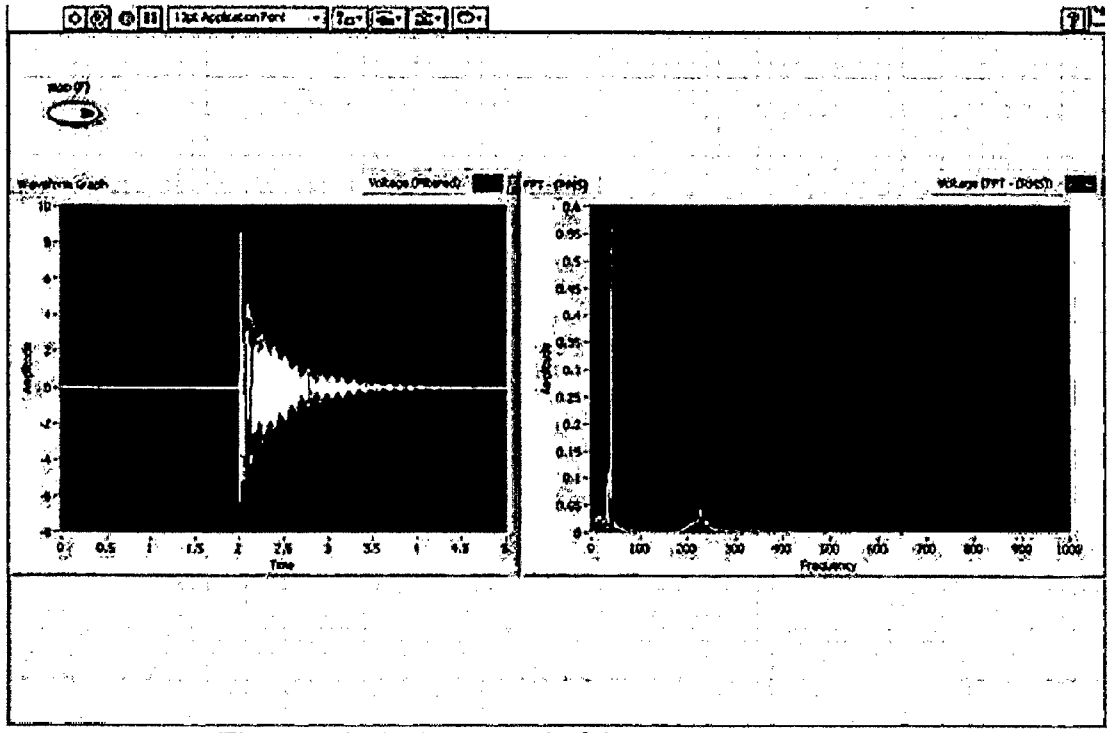

Figure 5.6 (a): Front panel of the LABVIEW VI program.

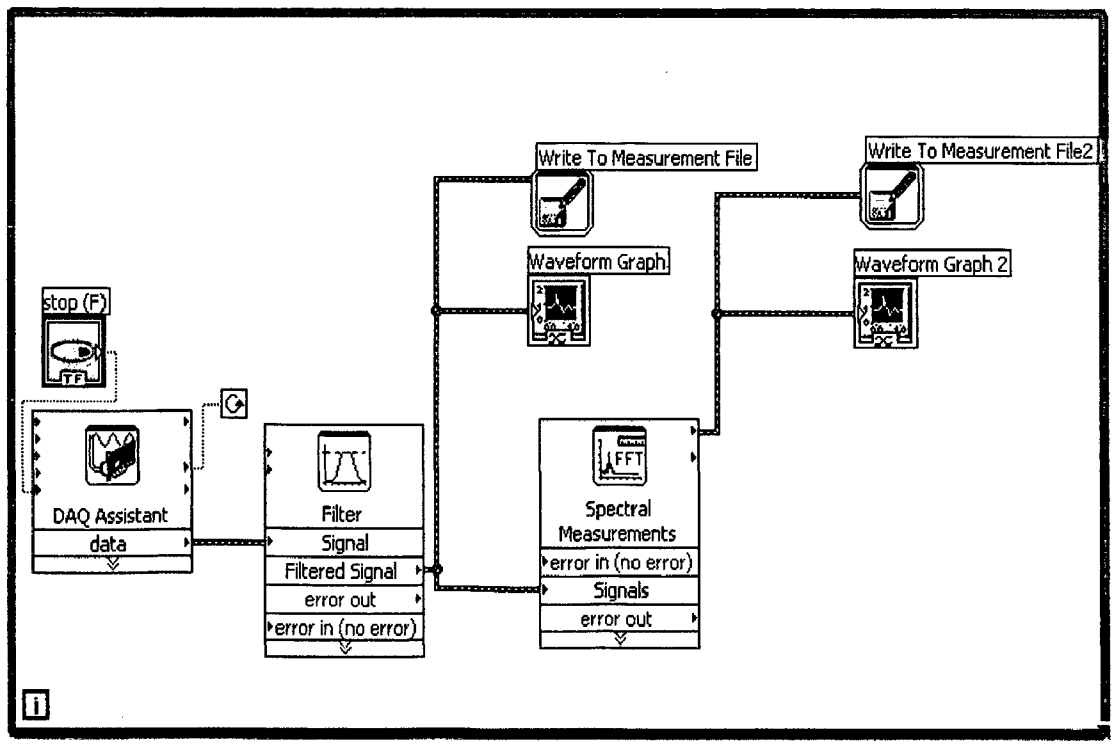

Figure 5.6 (b): Block diagram of the LABVIEW VI program.

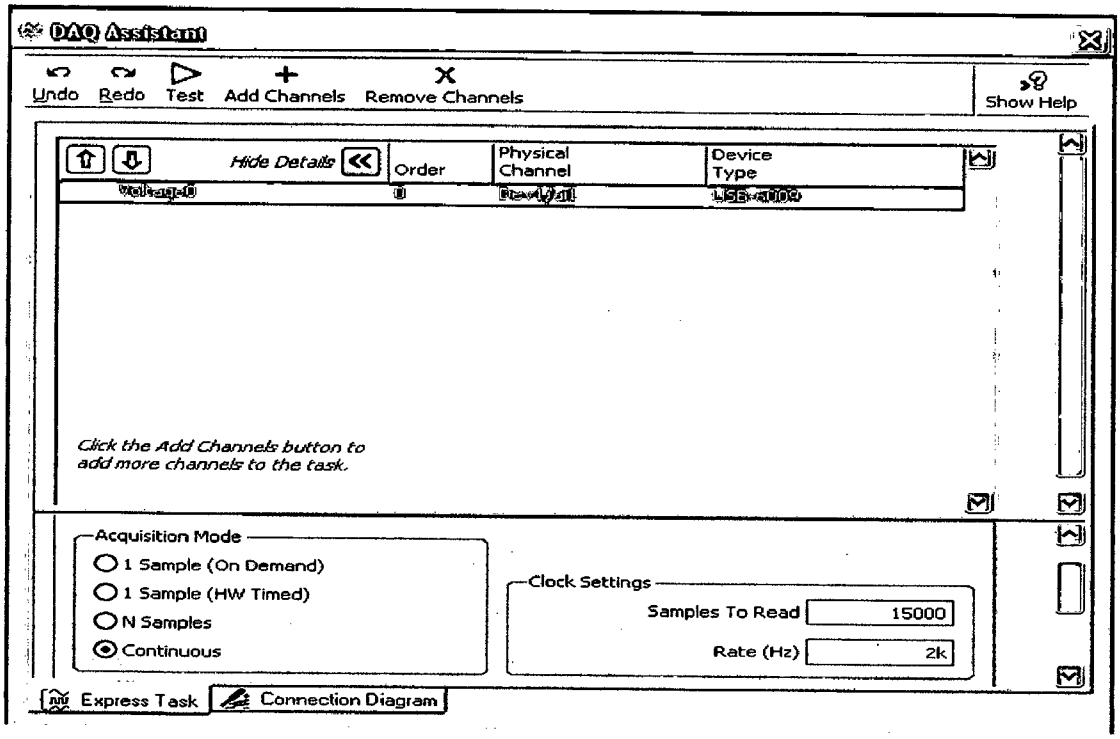

Figure 5.7: DAQ assistant parameter dialogue box.

5.3 Procedure

The proportional control method has been used for the vibration suppression Therefore the output of the sensor is given to the input of the actuation system directly after providing some gain (amplification). For performing the experiment, the semi-circular cylindrical shells are excited with random impulse manually. Sensed voltage is recorded in the PC without and with control gain by the actuation system. It implies that the data are stored without control action and with control action. Both data are then normalized with the sensor voltage. These normalized data are compared with each other on the same scale with different gain value. Following points are considered during the experiment.

(1) Aluminum semi-circular cylindrical shells with patch bonded on to the surface are placed properly on the clamping structure as shown in the figure 5.2.

(2) PZT patches are wired to the piezo sensing and actuation system properly.

(3) DAQ NI card is connected to the PC using USB cable. The output of the sensing system is transmitted to the proper analog input port of the NI card and input of the actuation system.

(4) BNC and coaxial wire connection is mostly used for the interconnection of all the devices to avoid shorting of wires and to reduce the noise level.

Chapter 6

RESULTS AND DISCUSSION

Shell structure with bonded piezoelectric layer to act as sensor and actuator are used by number of researcher and many discussions are made on it. This chapter consists of results and discussion on the present work includes static and dynamic validation of structure, optimal placement of patches and experimental results.

6.1 Validation of shell structure

6.1.1 Static validation

A semi circular cylindrical shell structure bonded with piezoelectric layer to act as sensor and actuator shown in figure 6.1 is loaded with different static loads at tip. Material properties used are given in table 5.1 and table 5.3.

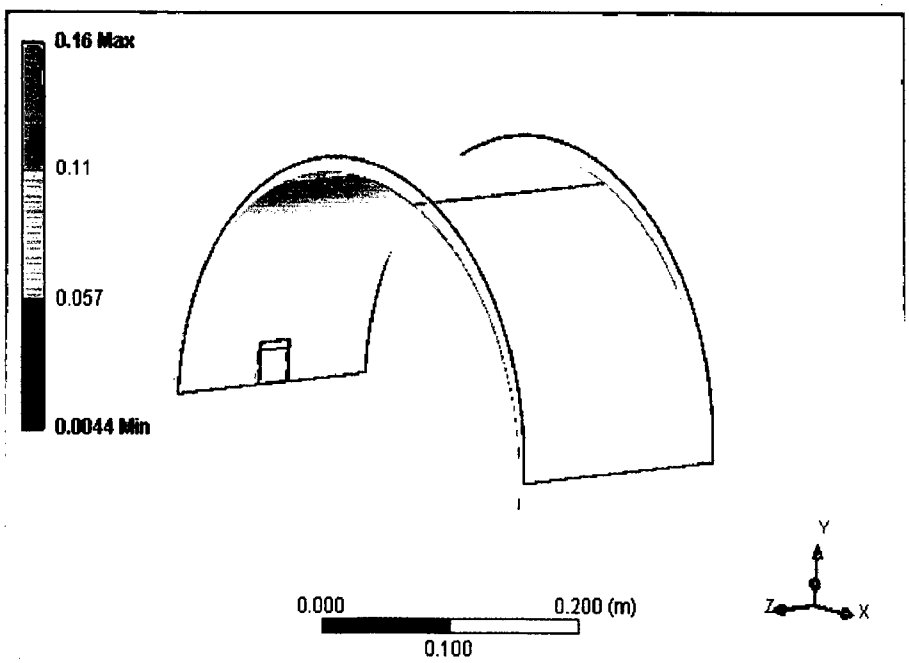

Figure 6.1: Shell structure bonded with piezoelectric layer.

The deflection of the tip is measured for each load and the results are validated with Ansys workbench results shown in table 6.1.

Table 6.1: Comparison of Ansys and experimental static results.

Load(N)	Ansys workbench Results(mm)	Experimental Results(mm)	% Error
0.025	0.57	0.62	8.06
0.05	0.74	0.82	9.76
0.075	0.11	0.12	8.33
0.1	1.6	1.8	11.1

The results agree very well with Ansys workbench results with an average error of 10%.The results are encouraging and the shell structure is used for further analysis. The conclusions of static validation are shown in figure 6.2.

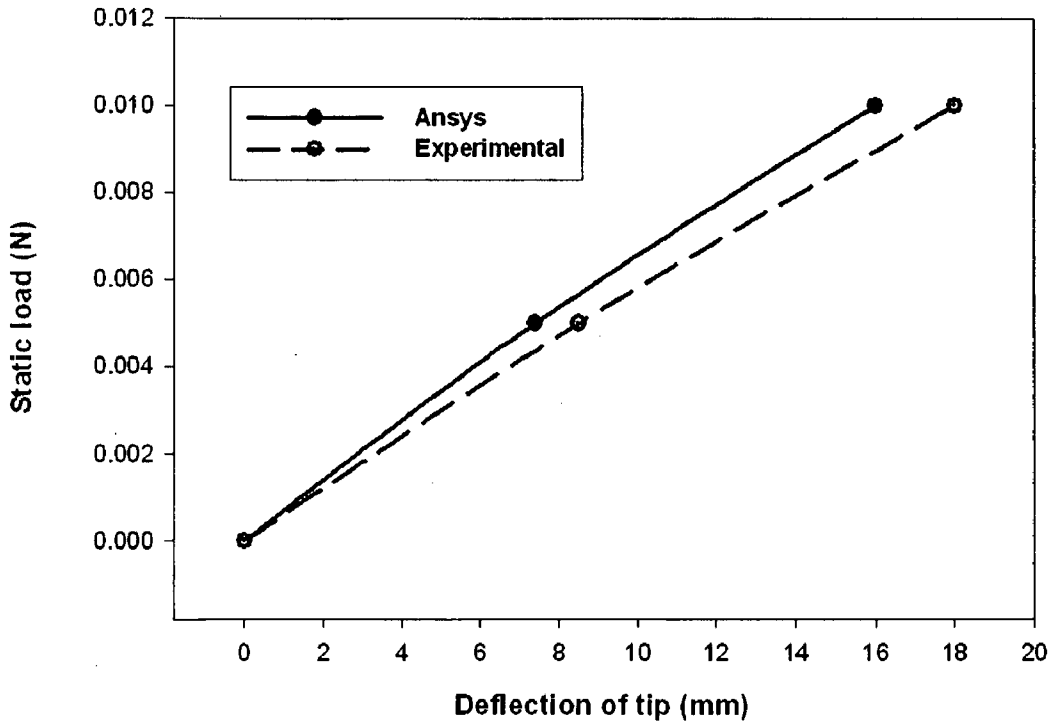

Figure 6.2: Conclusions of static validation.

6.1.2 Dynamic Validation

The dimensionless natural frequencies of the semi circular cylindrical cantilevered shell without piezoelectric patch is calculated form Ansys workbench shown in figure 6.3 and the results obtained are compared with the results obtained by Ye and Tzou. Comparison of first 3 natural frequencies is shown in the table 6.3. The

shell is 200 mm long, 150 mm wide, 0.8 mm thick and its inner radius is 63.66 mm. Material properties used are given in table 6.2.

Table 6.2: Material properties used for dynamic validation.

Properties	Steel	Unit
Young's modulus	0.21×10^{12}	Pa
Poisson ratio	0.3	
Density	7.8×10^{3}	Kg/m^3

Table 6.3: Comparison of first 3 natural frequencies.

Ansys workbench results	Ye and Tzou results	Error in %
46.302	37.87	10.41
135.53	138.55	2.2
437.09	471.27	7.33

The dynamic response obtained is quit satisfactory and it validates the sequence used in Ansys workbench for obtaining natuaral frequency of shell structure. These sequence can further used for analysis.

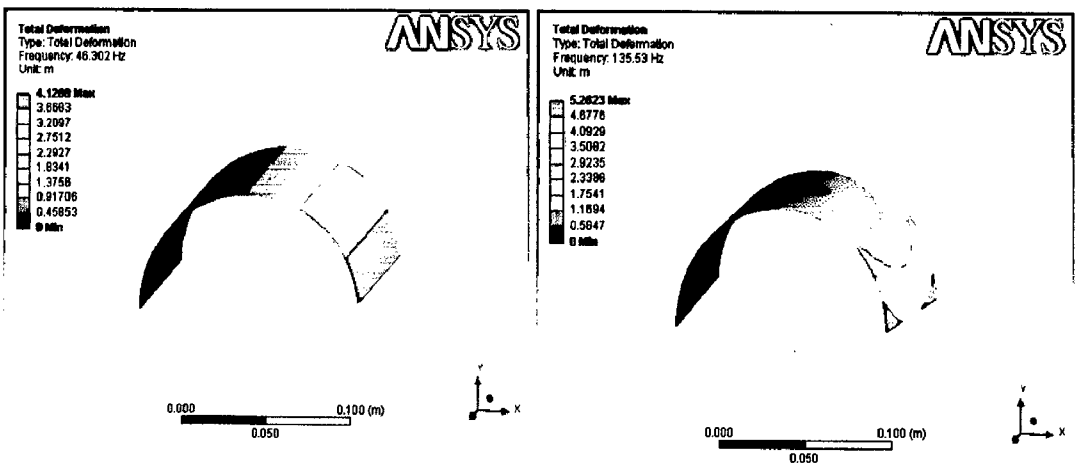

I Mode: f_n = 45.302 Hz

II Mode: f_n = 135.53 Hz

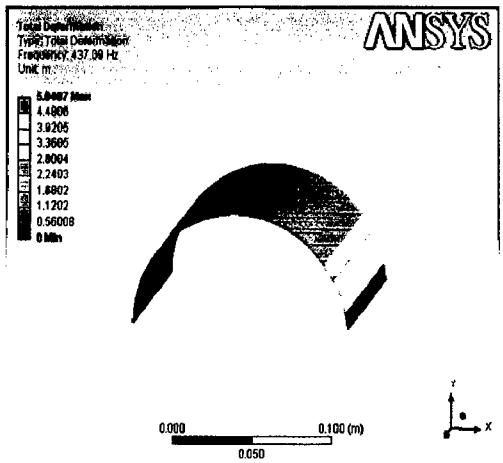

III Mode: f_n = 439.09 Hz

Figure 6.3: Natural frequencies of the semi circular cylindrical cantilevered shell.

6.2 Mode Shapes and Natural Frequencies

In this section, mode shapes and natural frequencies of the semi circular cylindrical cantilevered shell are presented considering the mass and stiffness of piezoelectric patches.

6.2.1 Semi circular cylindrical cantilevered shell

Figure 6.4 shows first six mode shapes and natural frequencies of the semi circular cylindrical cantilevered shell with two piezoelectric patches attached to it. One patch is attached at the fixed end on the centre line on the top surface and another symmetrically on the bottom surface.

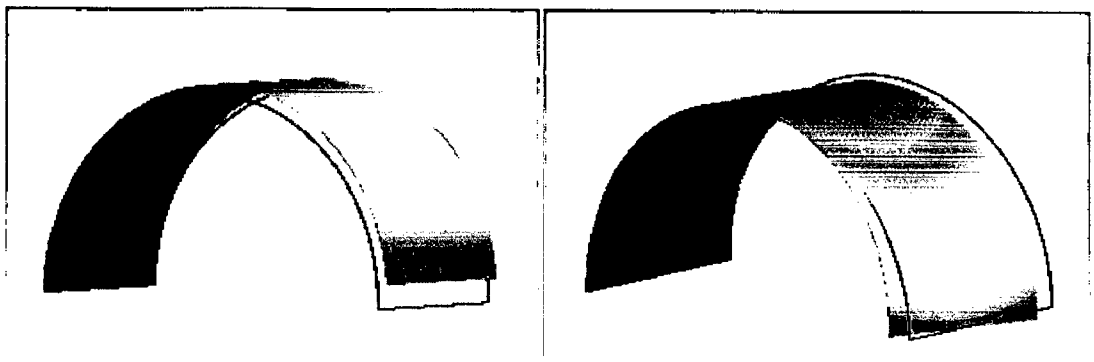

I Mode: f_n = 2.47 Hz

II Mode: f_n = 4.65 Hz

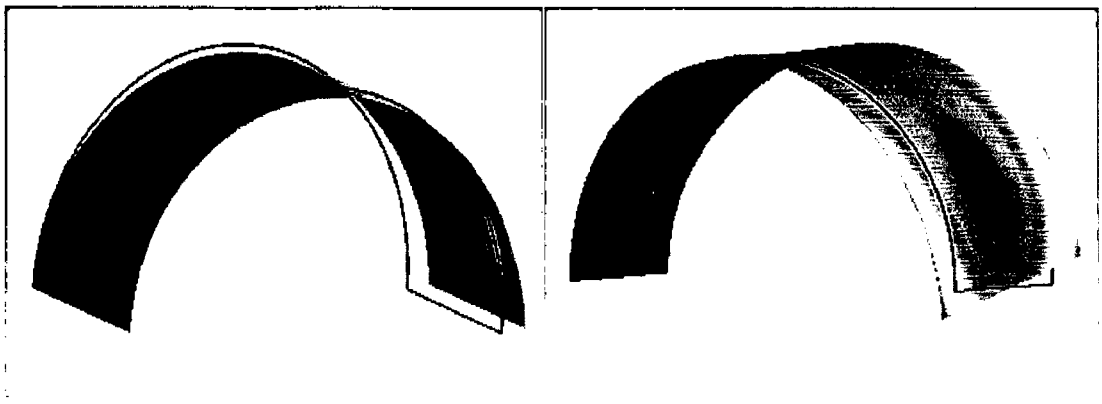

III Mode: f_n= 8.35 Hz

IV Mode: f_n= 20.41 Hz

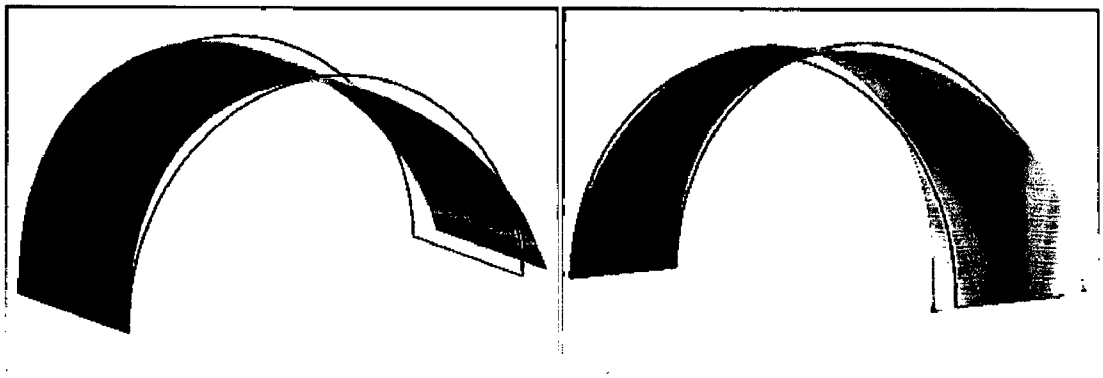

V Mode: f_n = 30.09 Hz

VI Mode: f_n = 51.08 Hz

Figure 6.4: Mode shapes and natural frequencies of the semi circular cylindrical cantilevered shell.

6.3 Optimum placement of sensor/actuator pair

The problem of optimal placement of sensor/actuator pair is of great importance as it is crucial in the robust functioning of the active control system. The optimization problem can be classified as continuous or discrete and the optimization method either non systematic like cut and try placement technique or systematic optimization method such as simulated annealing, tabu search and genetic algorithms. In the current work, pattern search method is used to obtain the optimum sensor/actuator position.

Hwang et al. suggested a design strategy for cantilevered structures with piezoelectric sensor and actuator pair and they observed that pairs closed to the fixed end are more effective then that of a pairs at free end. The start point for the pattern search is

selected based on the maxima of integrated normal strains that is sensors should be placed in regions where high integrated values of the normal strain over the bonding surface are located. In order to find starting point maximum normal strain for semi circular cylindrical shell is calculate with the help of Ansys workbench is shown in figure 6.5. Calculated results very well satisfy the observation made by Hwang et al.

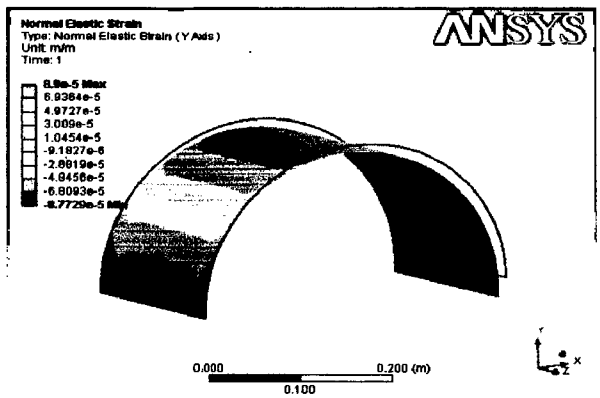

Figure 6.5: Normal strain in semi circular cylindrical shell.

Sensor and actuator pair is assumed to be collocated because actuator should always be placed in an area where the electric charge of the sensor is maximum. First starting point is assumed to be on centre line and results shows that a pair close to the fixed end is most effective in damping out the first mode whereas it is least effective at the free end. This conclusion agrees very well with the observation made by Hwang et al.

6.4 Setup performance

To know the performance of experimental setup first a square aluminum plate in cantilevered position is tested. The properties of the Al plate and PZT patch used in the experimental setup given in the table 6.4. Two PZT patches are bonded on the top and bottom surface of the plate in a symmetrical manner. Plate is excited by tapping and the sensor reading is recorded in the computer using the NI make data acquisition card. The results obtained are very encouraging shown in figure 6.6. The setup is enable to control the vibration, which quit satisfactory for further analysis.

Table 6.4: Properties of the aluminum plate and PZT

Property name	Aluminum	PZT (Sparkler Inc.)
Dimension (mm x mm x mm)	200 X 200 X 0.75	25 X 25 X 0.5
Young's modulus (N/m^2)	72E09	18.95E-9
Density (Kg/m^3)	2800	7500
Strain constant (d_{31})(m/V)	-	580E-12
Stress constant (g_{31}) (Vm/N)	-	0.020

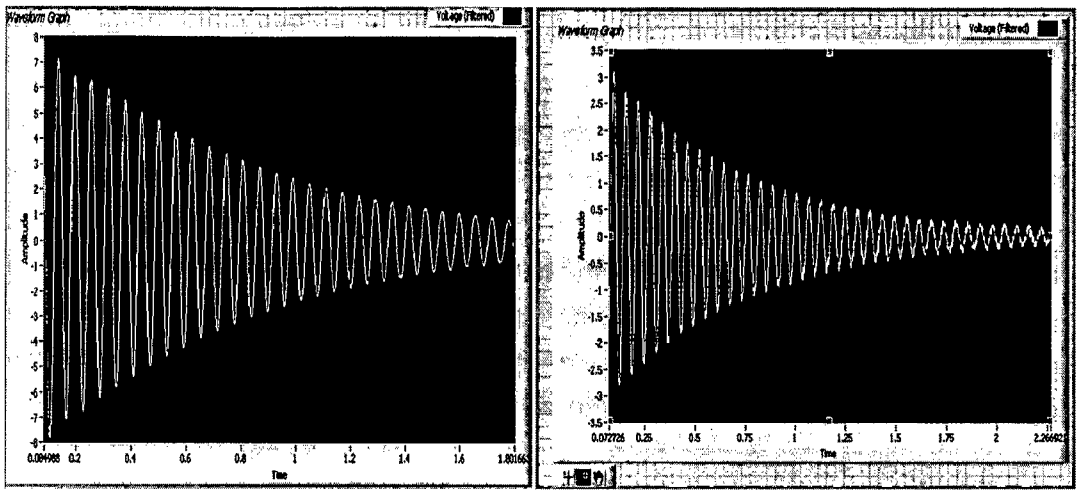

Figure 6.6: Uncontrolled and controlled response obtained from the experiment for first natural frequency of the plate.

6.5 Experimental results

In this section, the response of a semi circular cylindrical shell is obtained from experiment for the proportional feedback control for different values of control gain and the results obtained are quit satisfactory. The properties of the semi circular cylindrical shell and PZT patch used in the experimental setup given in the table 5.1 and 5.3 . Two PZT patches are bonded on the top and bottom surface of the semi circular cylindrical shell in a symmetrical manner. The semi circular cylindrical shell is excited by an impulse force at the free end near to the centre line of the semi circular cylindrical shell in order to vibrate the shell at first mode, the frequency of first mode is shown in figure 6.7. The sensor reading is recorded in the computer using the NI make data acquisition card. The sensor reading is taken during each impulse and the plot is compared with and

without the proportional control strategies. Here the sensor data is normalized for comparing the response with and without the control.

The theoretical calculated frequency for first mode is 2.5 Hz and is match very well with experimental frequency. Figures 6.8, shows uncontrolled response of shell for first mode and figure 6.9, 6.10 and 6.11 controlled response of shell for first mode obtained by experimentation at different gains 1, 2 and 5 respectively.

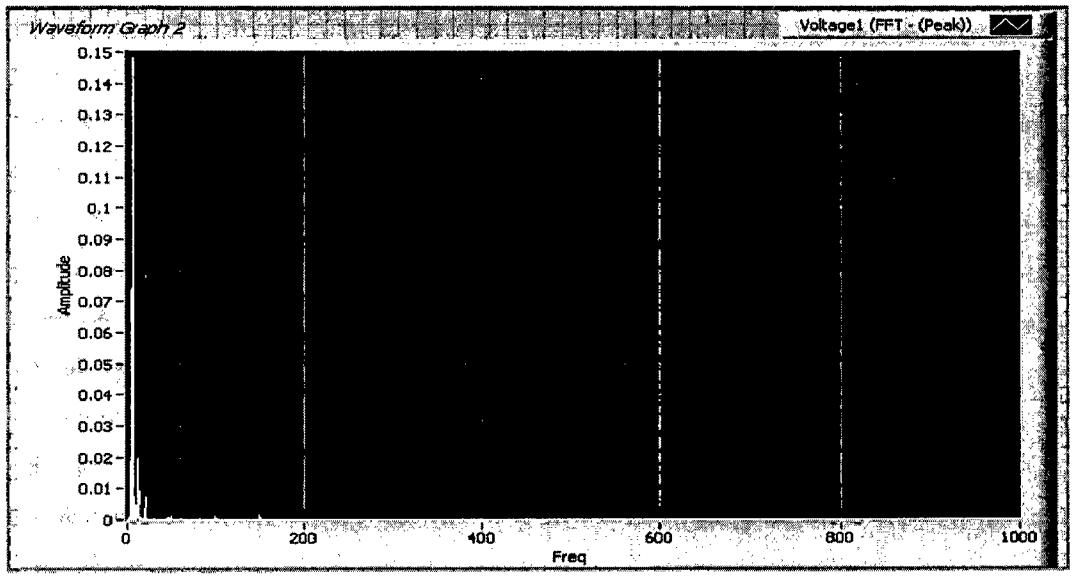

Figure 6.7: First mode natural frequency of shell.

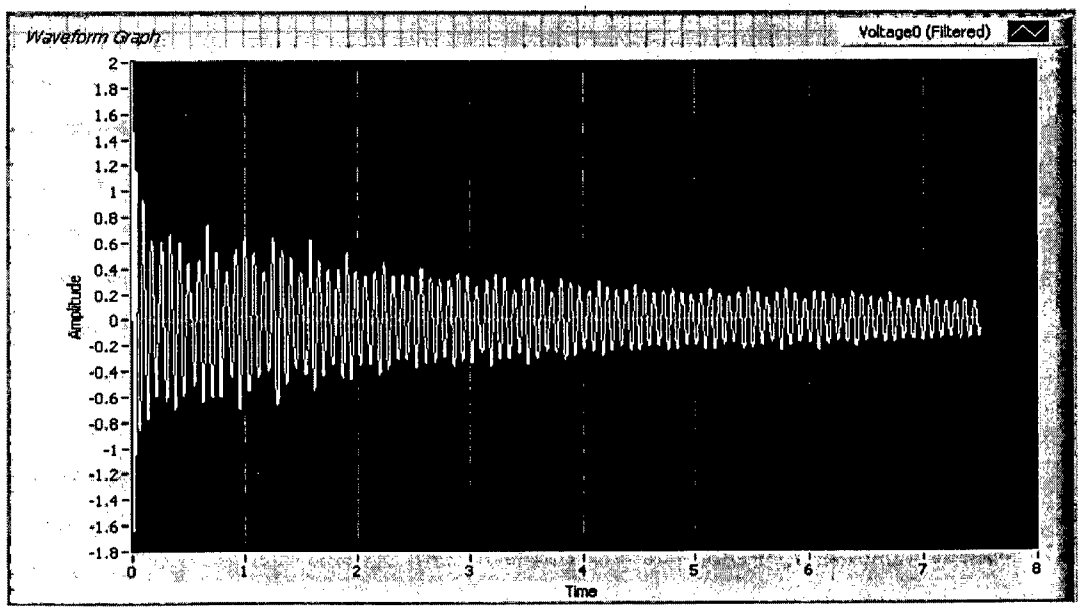

Figure 6.8: Uncontrolled sensor response.

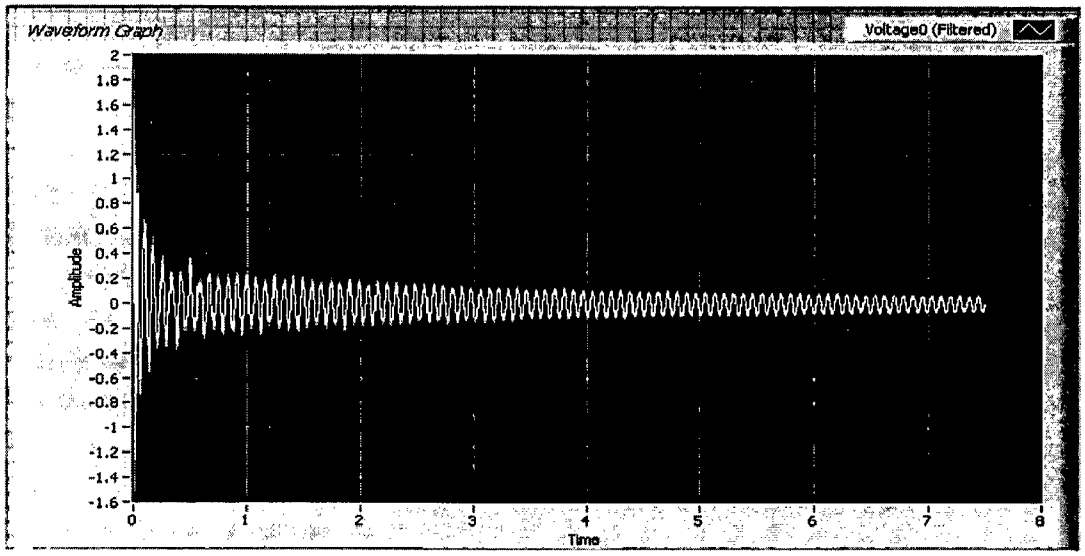

Figure 6.9: Controlled sensor response with gain 1.

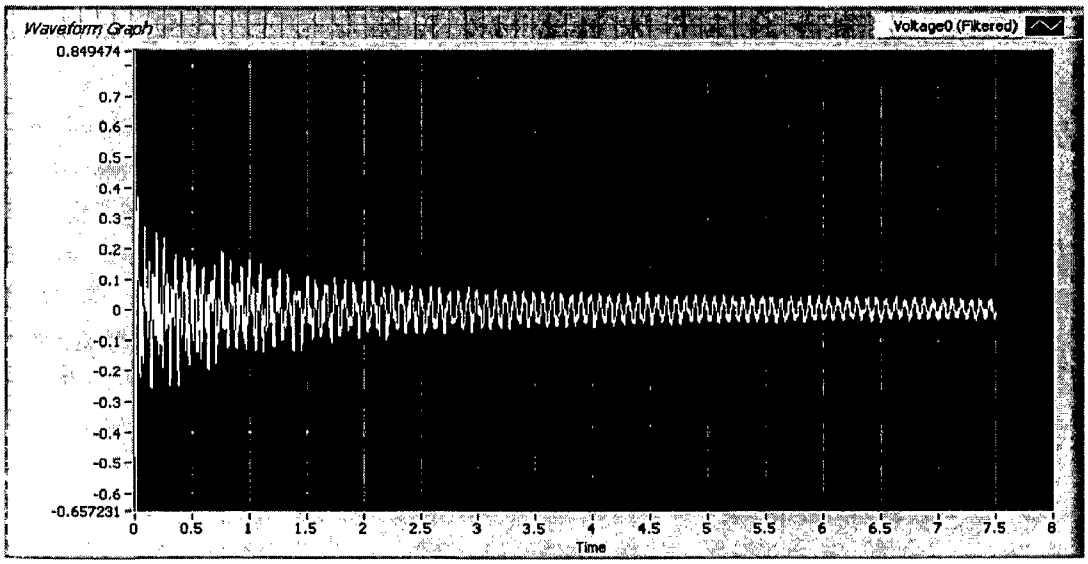

Figure 6.10: Controlled sensor response with gain 2.

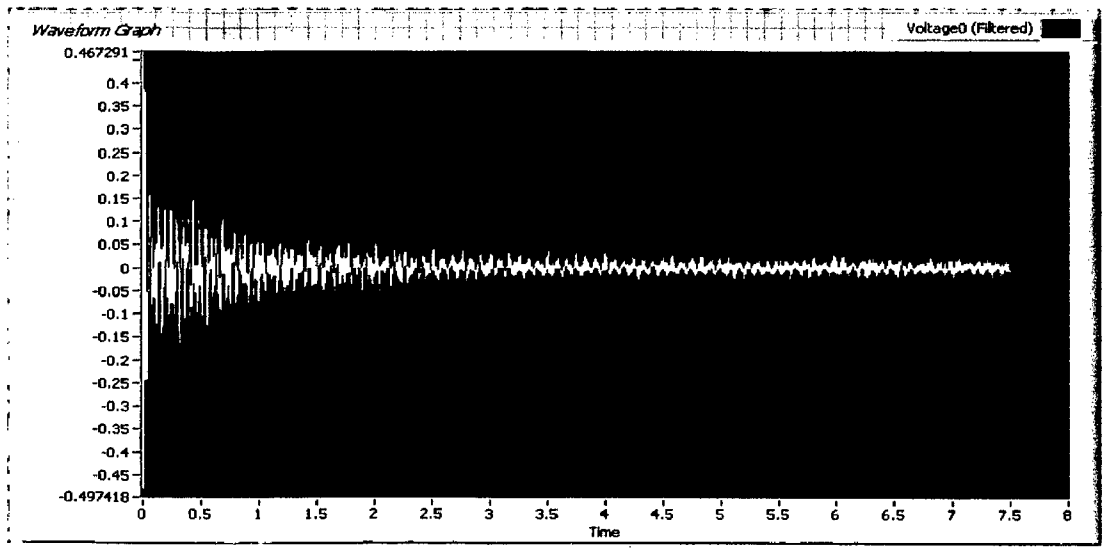

Figure 6.11: Controlled sensor response with gain 5.

It is observed that the damping effect increases with increase in control gain. Figure 6.12 shows the comparison for both uncontrolled and controlled response obtained from the experimentation for a semi circular cylindrical shell. As control gain is increasing, decay rate is also increasing; the first mode of vibration of semi circular cylindrical shell is best controlled at gain 5.

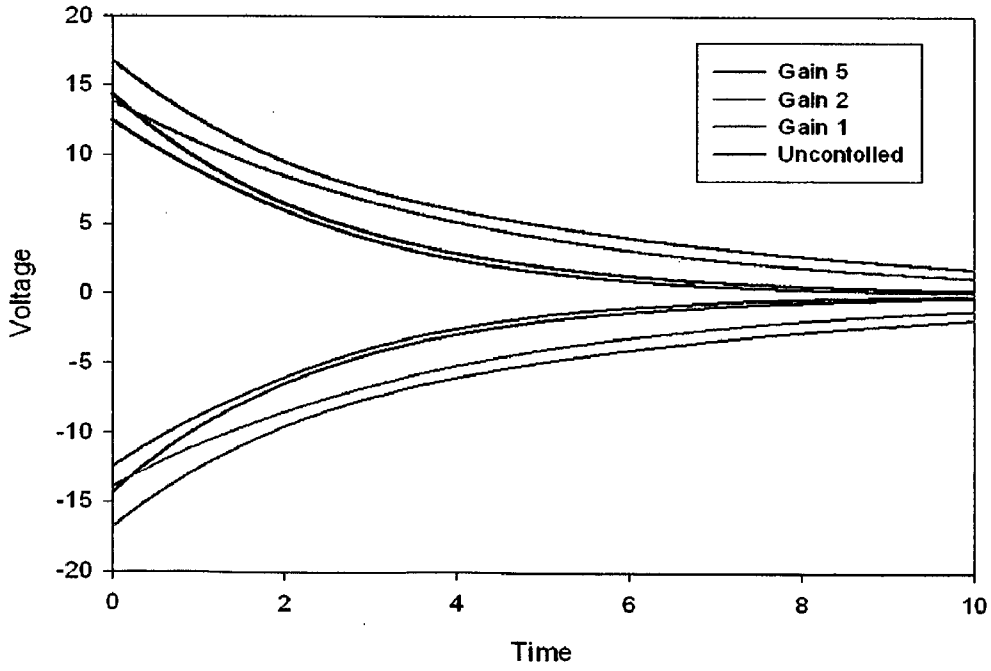

Figure 6.12: Uncontrolled and controlled sensor response with different gain.

Table 6.5 shows the comparison of the natural frequency of the semi circular cylindrical shell. It has been observed that the theoretical results of the present work compares very well with the experimental results.

Table 6.5: Comparison of Natural frequency of semi circular cylindrical shell.

Sr. No.	Theoretical (Hz)	Experimental(Hz)	Error (%)
1	2.47	2.2	10.93
2	4.65	4.3	7.52
3	8.35	8.5	1.8
4	20.41	21	2.89

The actuator response at gain 1, 2 and 5 is giving in figure 6.13, 6.14 and 6.15 respectively. Actuator response is increasing with increase in gain.

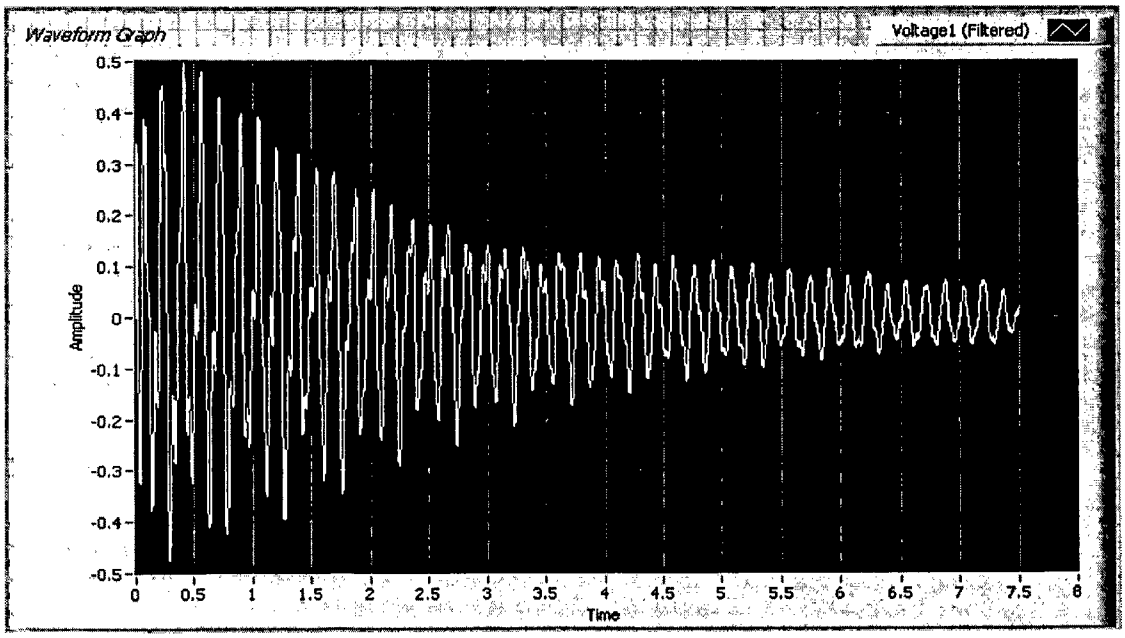

Figure 6.13: Actuator response with gain 1.

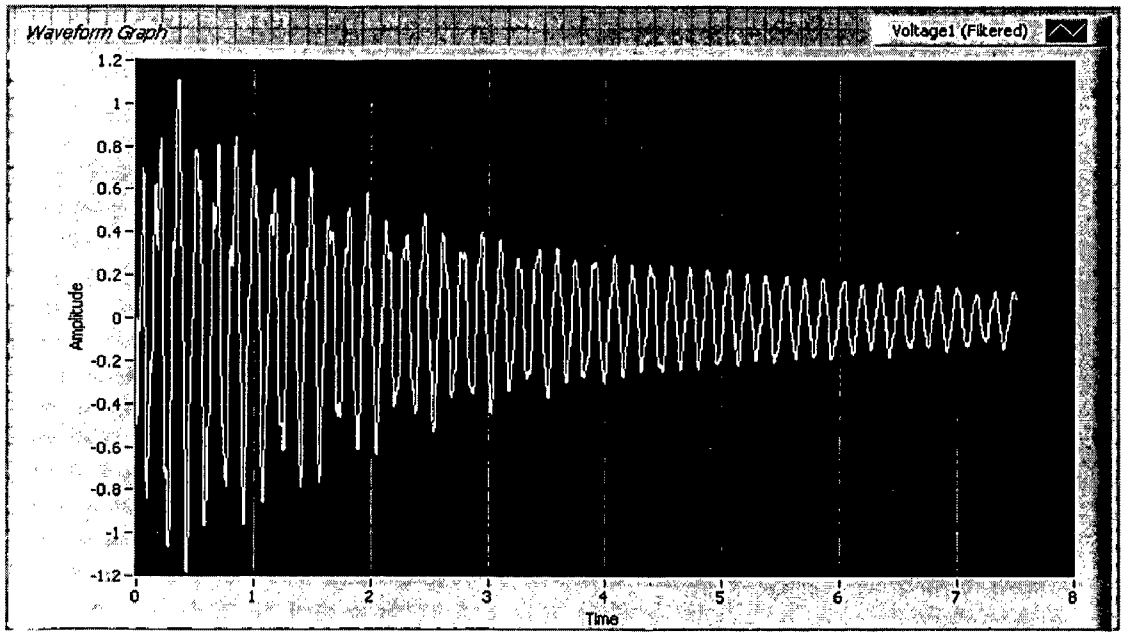

Figure 6.14: Actuator response with gain 2.

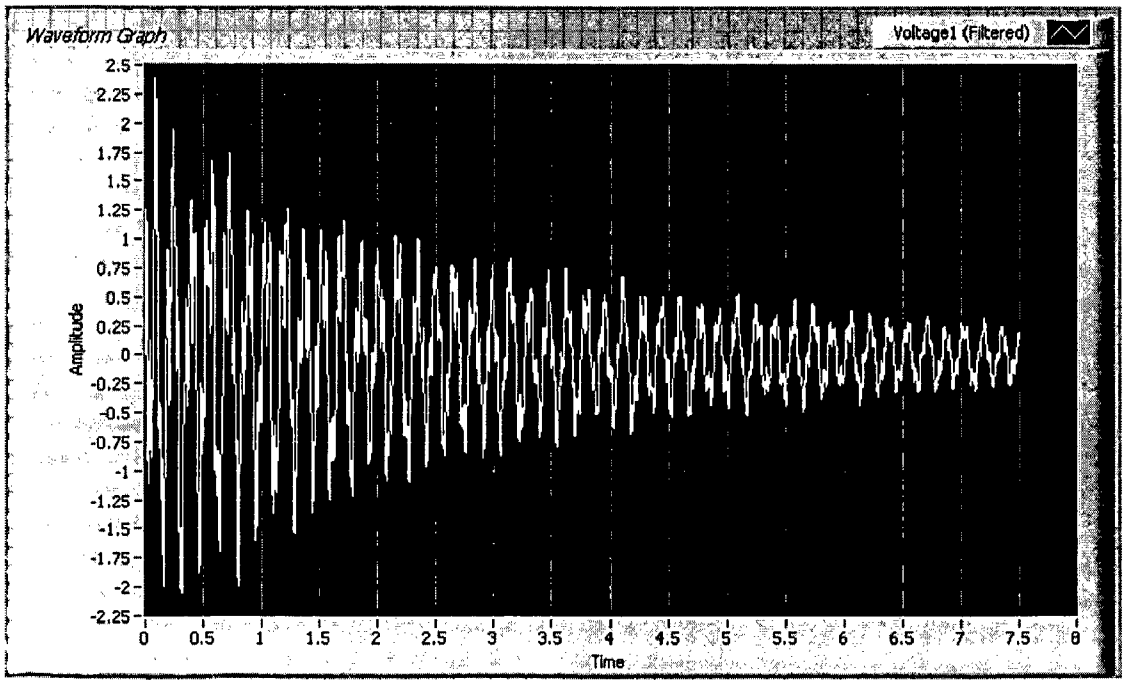

Figure 6.15: Actuator response with gain 5.

Chapter 7

CONCLUSION AND FUTURE SCOPE

7.1 Conclusion

The experimental setup consists of a piezo voltage amplifier and a data acquisition card. The aluminum shell with bonded piezoelectric ceramic sensor and actuators is excited. The sensor reading is taken and stored into computer using the LabVIEW software and DAQ hardware interface.

The natural frequency (FEM) of the shell is validated with the experimental frequency. The uncontrolled and controlled response obtained by experimental setup. From the numerical and the experimental results obtained in the current work, following conclusions are drawn:

- It is observed that the vibration suppression increases as the actuator gain increases. It is because of greater controlling force.
- In the case of the proportional control method with the particular gain amplitude of vibration decays due to effective stiffness.
- Damping effect varies considerably with the position of piezoelectric patches on the surface of the patch. Hence it is very important to place the patches at the most effective position to obtain the maximum suppression in the amplitude of vibration.
- Natural frequency of a semi circular cylindrical shell increases when the piezoelectric patch is mounted on it. It is because of the addition of a material with higher stiffness : mass ratio to the original structure.
- The damping effect increases with increase in control gain. The practical limit of the control gain depends on the breakdown voltage of the piezoelectric material.
- Experiments demonstrate that the piezoelectric sensors can accurately and effectively obtain the natural frequencies of the structure and the proportional control can achieve active vibration control damping of the shell with piezoelectric ceramics patches as both sensor and actuator.

7.2 Scope for future work

- Investigation on the shell structure with different boundary condition can be carried out to find the effectiveness of the method.
- Experiments can be performed changing the control algorithm on the same structure for example velocity feedback, integral or combinations of them.
- Similar analysis can be performed to obtain the suppression of higher mode vibrations by changing the position of the patch.
- The effect of adhesive layer between the plate surface and the patch structure can be considered in the numerical formulation.
- Analysis can be performed for more number of patches attached to the structure.
- Similar analysis can be performed for change in the operation mode, i.e. use of piezo sensing and actuation system can be completely replaced with the help of a computer with input output interface device or PZT can be replaced with other sensing device like MFC.
- Analysis to predict accurately the behavior of sensor and actuator when used with composite beams, plates and shells.

REFERENCES

1. **Aida T, Aso T and Nakamoto K**, "Vibration control of shallow shell structure using a shell type dynamic vibration absorber", Sound and Vibration, vol 218, 1998, pp 245- 267.

2. **Akella Padma, Chen Xin, Cheng Weiying, Hughes Declan and T Wen John**, "Modeling and control of smart structures with bonded piezoelectric sensors and actuators" ,Smart Mater. Struct. Vol 3, 1994, pp 344-353.

3. **Ansari R and Darvizeh M**, "Prediction of dynamic behaviour of FGM shells under arbitrary boundary conditions", Composite Structures, vol 85, 2008, pp 284–292.

4. **Awrejcewicza J and Kryskob V A**, "Some problems of analysis and optimization of plates and shells", Sound and Vibration, vol 264, 2003, pp 343–376.

5. **Balamurugan and Narayanan**, "A piezolaminated composite degenerated shell finite element for active control of structures with distributed piezosensors and actuators", Smart Material Structure, vol 17, 2008, pp 18-35.

6. **Barrault Guillaume, Halim Dunant, Hansen Colin and Lenzi Arcanjo**, "High frequency spatial vibration control for complex structures", Applied Acoustics, vol 69, 2008, pp 933–944.

7. **Berg M, Hagedorn P and Gutschmidt S**, "On the dynamics of piezoelectric cylindrical shells", Sound and Vibration, vol 274, 2004, pp 101–109.

8. **Brennan M J, Day M J, Elliot S J and Pinnington R J**, "The active vibration control", International Union of Theoretical and Applied Mechanics, Symposium, University of Bath, UK, 1994, pp 263-274.

9. **Bronowicki A J, McIntyre L J, Betros R S and Dvorsky G R**, "Mechanical validation of smart structures", Smart materials and structures, vol 5, 1995, pp 129-139.

10. **Chandrupatla T R and Belegundu A D**, Introduction to finite element in engineering, Pearson Education, III Edition, 2006, pp 23-38, 51-58, 230-240.

11. **Crawley E F and Lazarus K B**, "Indused strain actuation of isotropic and anisotropic plate", AIAA Journal, vol 29, 1991, pp 944-952.

12. **Crawley E F and Luis Javier de**, "Use of piezoelectric actuators as elements of integrated structure", AIAA Journal, vol 25, 1987, pp 1373-1385.

13. **Grover G K**, Mechanical Vibrations, Nem Chand and Bros Publications, VII Edition, 2003, pp 61-80, 249-263.

14. **Halim Dunant and Cazzolato Ben S**, "A multiple-sensor method for control of structural vibration with spatial objectives", journal of sound and vibration, vol 296, 2006, pp 226-242.

15. **Halim Dunant and Moheimani S O Reza**, "An optimization approach to optimal placement of collocated piezoelectric actuators and sensors on a thin plate", Mechatronics, Vol 13, 2003, pp 27-47.

16. **Han J H, Rew K H and Lee In**, "An experimental study of active vibration control of composite structures with a piezo-ceramic actuator and a piezo-film sensor", Smart material and structure, vol 6,1997, pp 549-558.

17. **Harris C M and Crede C E**, "Shock and Vibration Handbook", Mc-Graw hill book company, II Edition, 1976, pp 1.13-1.16, 7.26-7.32.

18. **Hiramoto K, Doki H and Obinata G**, "Optimal sensor/actuator placement for active vibration control using explicit solution of algebraic Riccati equation", Journal of sound and vibration, Vol 229, 2000, pp 1057-1075.

19. **Hwang W. S, Hwang W and Park H. C**, "Vibration control of laminated composite plate with piezoelectric sensor/actuator: Active and passive control method", Mechanical system and signal processing, vol 8, 1994, pp 571-583.

20. **Keir John, Kessissogolu Nicole J and Norwood Chris J**, "Active control of connected plates using single and multiple actuators and error sensors", Journal of sound and vibration, Vol 281, 2004, pp 73-97.

21. **Kumar Rajeev**, "Shape and vibration control of smart structure", Doctoral thesis, IIT Roorkee, 2007

22. **Kurpaa Lidia, Pilguna Galina and Amabilib Marco**, "Nonlinear vibrations of shallow shells with complex boundary: R-functions method and experiments", Sound and Vibration, vol 306, 2007, pp 580–600.

23. **Lee Won-Hong and Cheon Sung**, "Free and forced vibration analysis of laminated composite plates and shells using a 9-node assumed strain shell element", Comput. Mech. , vol 39, 2006, pp 41–58.

24. **Lee Y Y and Yao J**, "Structural Vibration suppression using the piezoelectric sensors and actuators", Journal of Vibration and Acoustics, Vol 125, 2003, pp 109-113.

25. **Mehrdad Ghasemi-Nejhad** , Russ Richard and Pourjalali Saeid, "Manufacturing and testing of active composite panels with embedded piezoelectric sensors and actuators", Journal of intelligent material systems and structures, vol 16, 2005, pp 319-333.

26. Mustafa B A J and Ali R,"Prediction of natural frequency of vibration of stiffened cylindrical shells and orthogonally stiffened curved", Sound and Vibration, vol 113, 1987, pp 317-327.

27. Nagaia K, Maruyamaa S, Muratab T and Yamaguchi T, "Experiments and analysis on chaotic vibrations of a shallow cylindrical shell-panel", Sound and Vibration, vol 305, 2007, pp 492–520.

28. Narayanan S and Balamurugan V, "Finite element modeling of piezolaminated smart structures of active vibration control with distributed sensors and actuators", Journal of sound and vibration, vol 262, 2003, pp 529-56.

29. Obe O. Ibidapo, "Optimal actuators placements for the active control of flexible structures", Journal of mathematical analysis and applications, Vol 105, 1985, pp 12-25.

30. Park Gyuhae, Ruggiero Eric and Inman Daniel J, "Dynamic testing of inflatable structures using smart materials", Smart Material and Structure, vol 11, 2002, pp 147–155.

31. Qiu Jinhao and Haraguchi Masakhazu, "Vibration control of a plate using a self-sensing piezoelectric actuator and an adaptive control approach", Journal of intelligent material systems and structures, vol 17, 2006, pp 661-669.

32. Quek S T, Wang S Y and Ang K K, "Vibration control of composite plate via optimal placement of piezoelectric patches", Journal of intelligent materials and structures, vol 14, 2003, pp 229-245.

33. Roy Tarapada and Chakraborty Debabrata, "Optimal vibration control of smart fiber reinforced composite shell structures using improved genetic algorithm", Sound and Vibration, vol 319, 2009, pp 15–40.

34. Smithmaitrie P, Tzou H S, "Micro-control actions of actuator patches laminated on hemispherical shells", Sound and Vibration, vol 277, 2004, pp 691–710.

35. Thomson B S, Gandhi M V and Kasiviswanathan S,"An introduction to smart materials and structures", Materials and Design, Vol 13, 1992, pp 3-9.

36. Tzou H S, "A new distributed sensor and actuator shell theory for intelligent shell" , Sound and Vibration, vol 153, 1992, pp 335-349.

37. Tzou H S , Bao Y. and Venkayya V B, "Parametric study of segmented transducers laminated and cylindrical shell", Sound and Vibration, vol 197, 1996, pp 225-249.

38. Tzou H S and Ding J H, "Optimal control of precision paraboloidal shell structronic systems", Sound and Vibration, vol 276, 2004, pp 273–291.

39. Van H Nguyen, Mai-Duy N and Tran-Cong T, "Free vibration analysis of laminated plate/shell structures based on FSDT with a stabilized nodal-integrated quadrilateral element", Sound and Vibration, vol 313, 2008, pp 205–223.

39. Verma Amit, "Active vibration control of plate", Master thesis, IIT Roorkee, 2008.

40. Ye R and Tzou H S, "Control of adaptive shells with thermal and mechanical exitation", Sound and vibration, vol 231, 2000, pp 1321-1338.

41. Young P G, "Application of 3D shell theory of free vibration of shell arbitrarily deep in one direction", Journal of Sound and Vibration, vol 238, 2000, pp 257-269.

42. Yue H H, Deng Z Q and Tzou H S, "Distributed signal analysis of free-floating paraboloidal membrane shells", Sound and Vibration, vol 304, 2007, pp 625–639.

43. Yue H H, Deng Z Q and Tzou H S, "Optimal actuator locations and precision micro-control actions on free paraboloidal membrane shells", Communications in Nonlinear Science and Numerical Simulation, vol 13, 2008, pp 2298–2307.

44.Zhang Yahong, Niu Hongpan, Xie Shilin and Zhang Xinong,"Numerical and experimental investigation of active vibration control in a cylindrical shell partially covered by a laminated PVDF actuator", Smart Mater. Struct., vol 17,2008, pp 12-24.